

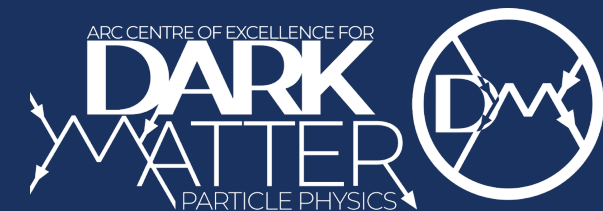


# DIRECT DETECTION OF DARK MATTER WITH THE SABRE SOUTH EXPERIMENT

Madeleine J. Zurowski

The University of Melbourne  
The University of Toronto

[madeleine.zurowski@utoronto.ca](mailto:madeleine.zurowski@utoronto.ca)

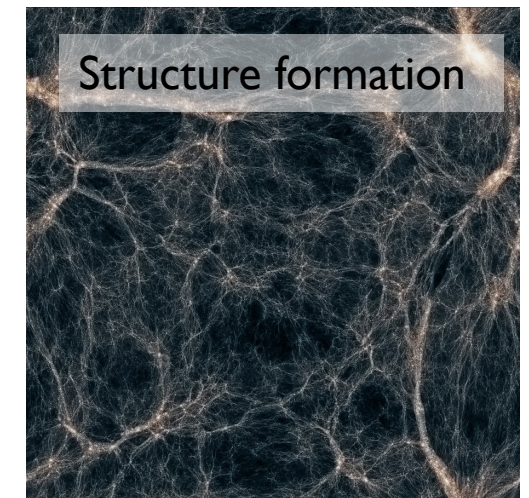
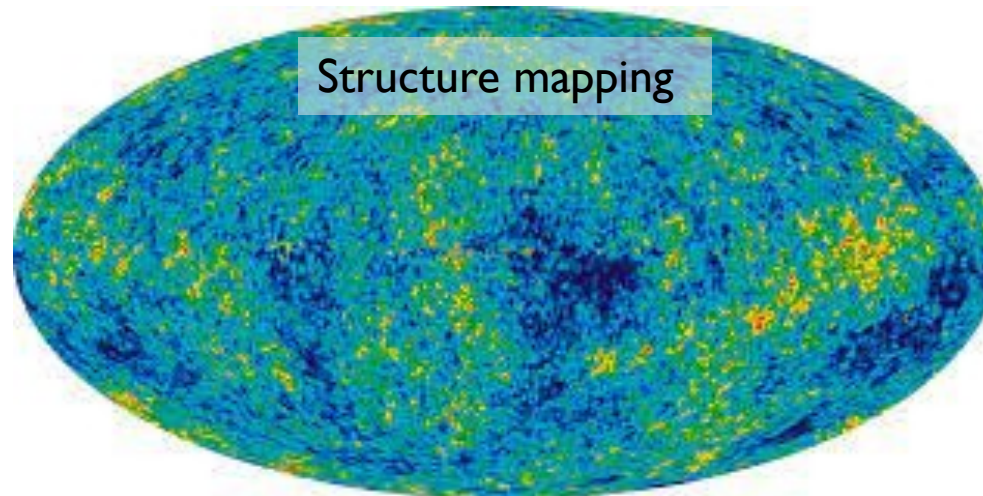
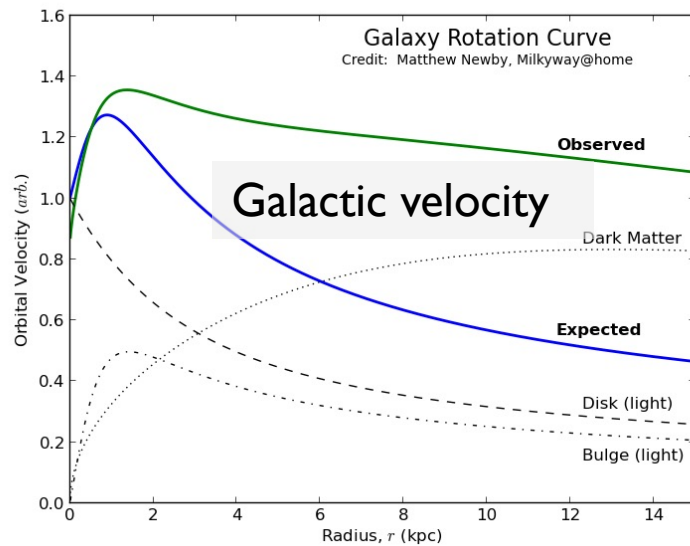
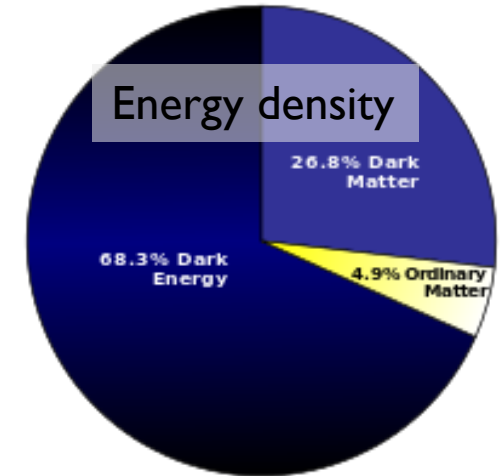
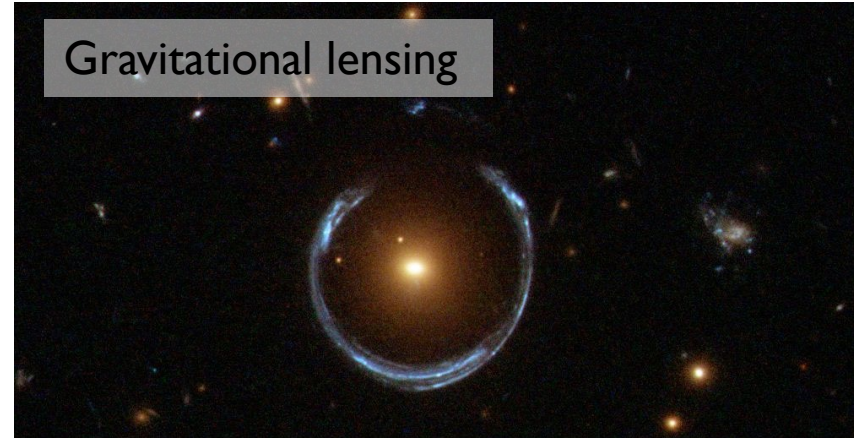
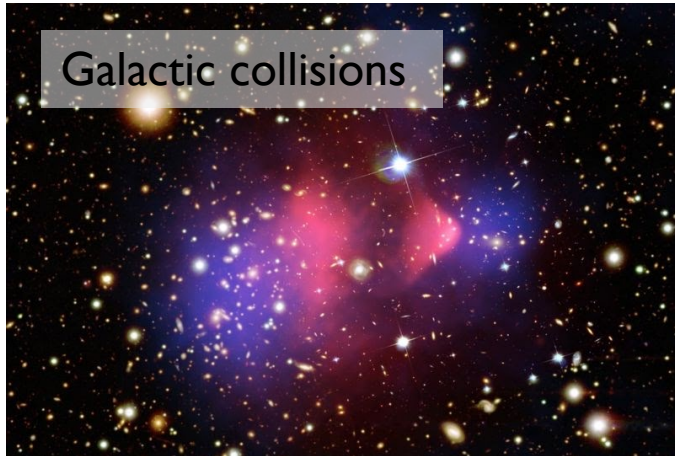


# KEY QUESTIONS TO ANSWER

- What is the DAMA experiment?
- How do we compute DM rates in detectors and compare results from different experiments?
- How can we thoroughly and efficiently test the DAMA modulation?
- What is SABRE? How is it expected to perform?



# DM EVIDENCE



# MODULATING SIGNAL

Astrophysical predictions of DM distribution imply a modulating signal due to Earth's rotation around the Sun.

$$R(E) = R_0(E) + R_m \cos(\omega(t - t_0))$$

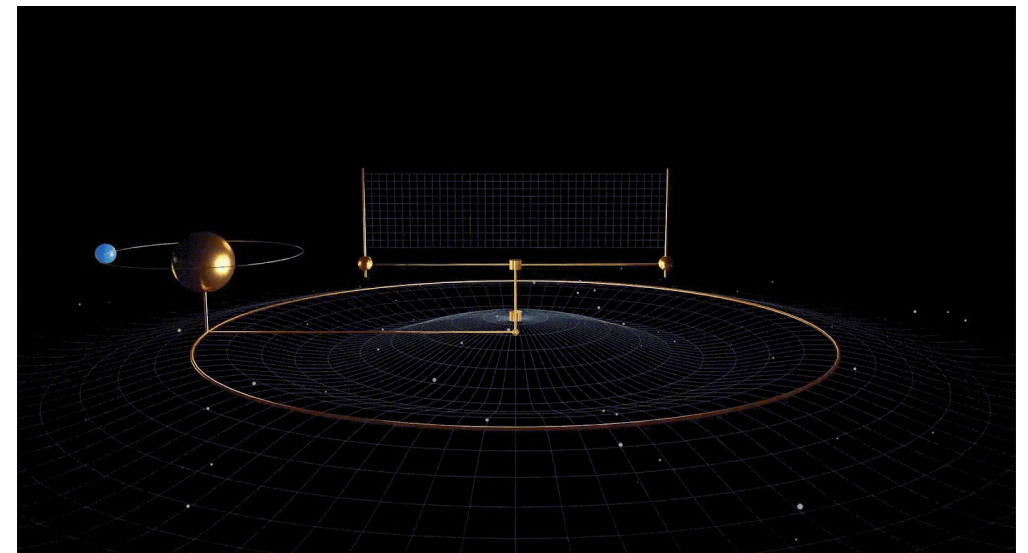
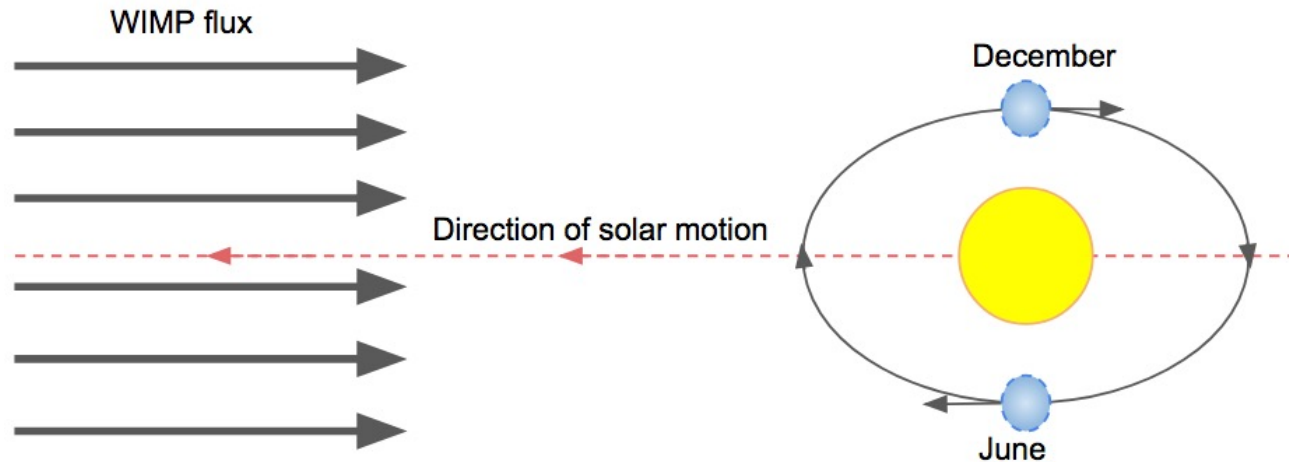
Period should be 1 year

Phase should produce a peak in June

Signal should appear in keV energy range

Events should be single hit

Signal should be identical in north and south hemispheres



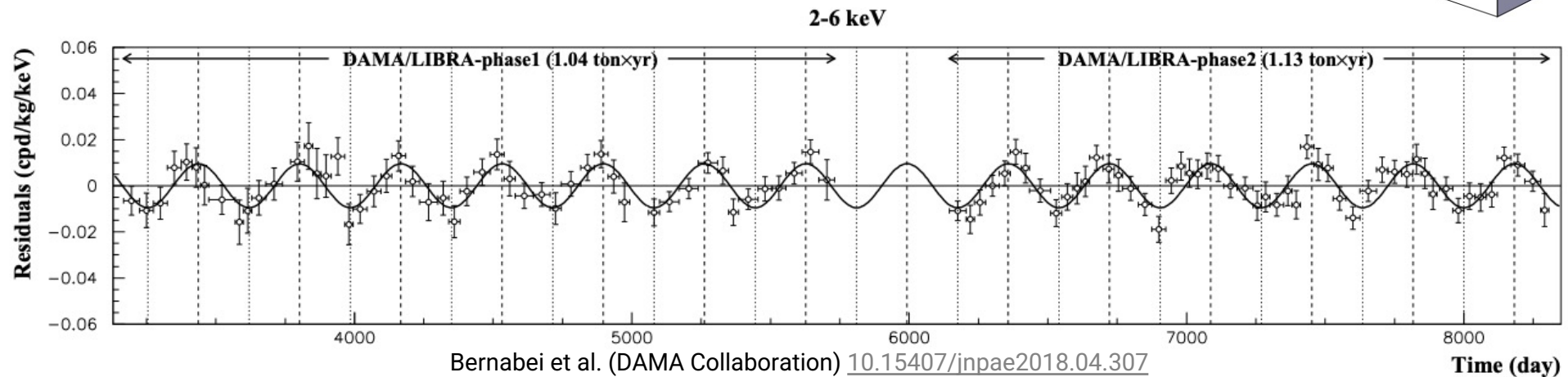
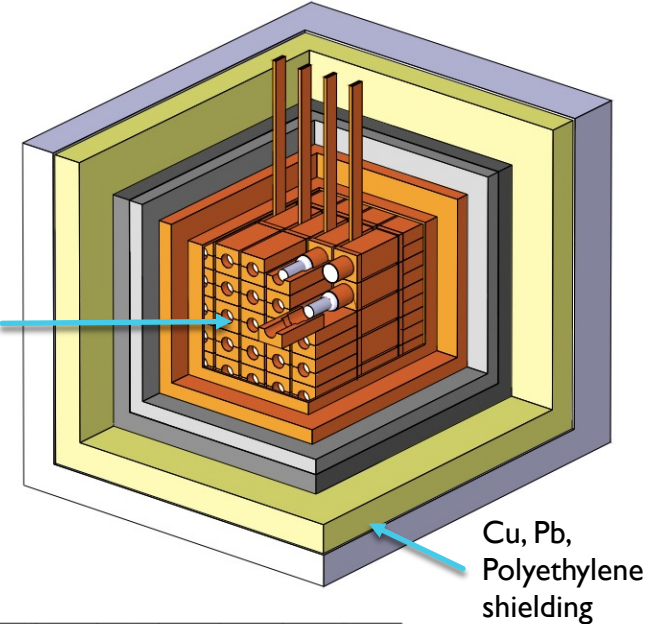
Olena Shmahalo / Quanta Magazine

# DAMA RESULTS

250 kg NaI(Tl) detector based in LNGS consistently observed modulation rate compatible with DM expectations for  $\sim 20$  years w/  $\sim 13\sigma$  CL

- $R_m: 0.01058 \pm 0.00090$  cpd/kg/keV
- Phase:  $144.5 \pm 5.1$  days
- Period:  $0.999 \pm 0.001$  yr
- Modulation present in 1-6 keV

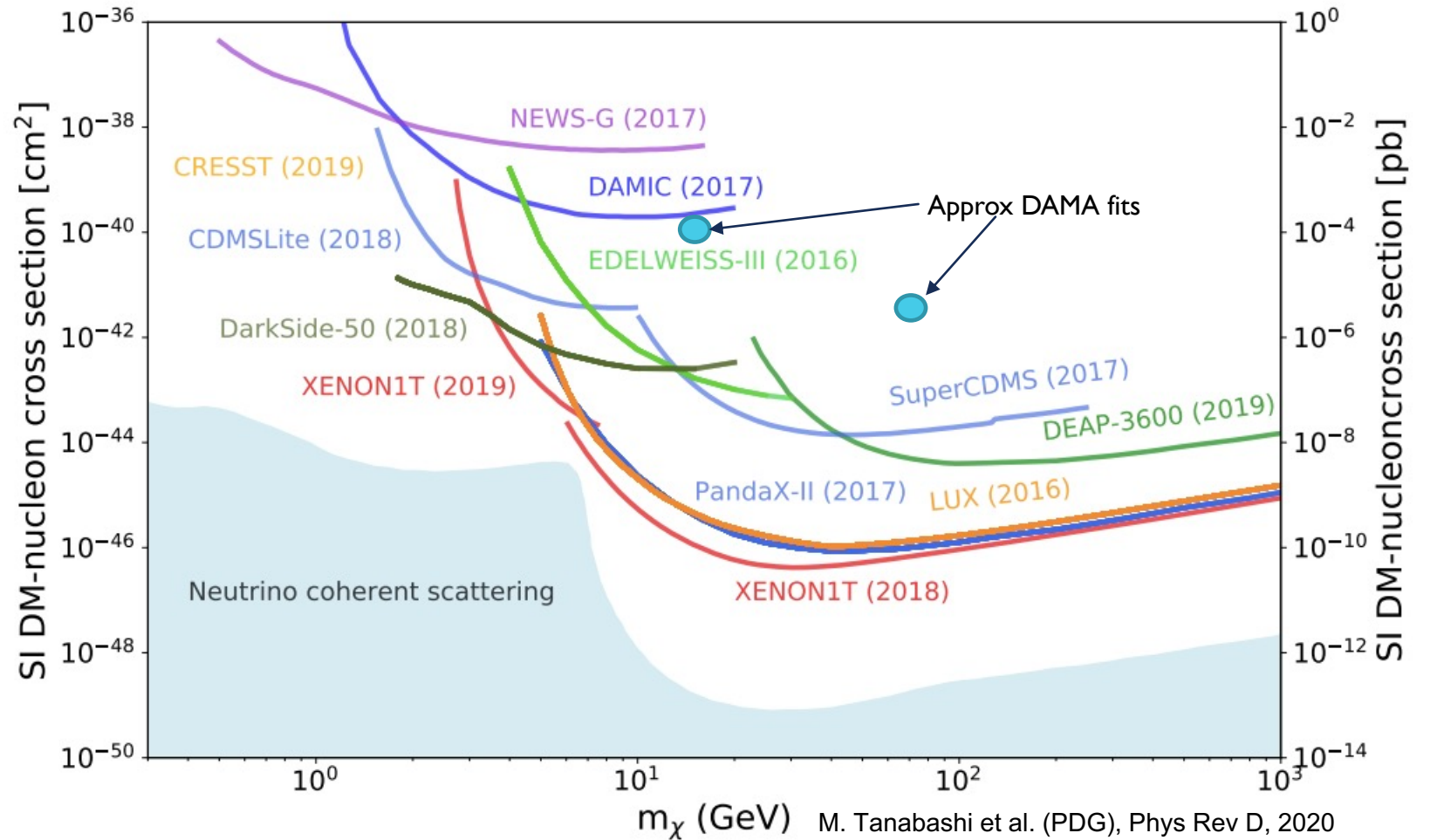
No direct fitting to constant rate, but upper limit given of  $\sim 0.8$  cpd/kg/keV



# EXPERIMENTAL TENSION

Interpretation as DM is strongly constrained by null results from different targets

Target	Experiment/s
O	CRESST
F	PICO, PICASSO
Ne	NEWS-G
Na	DAMA
Si	DAMIC
Ar	DEAP, DarkSide
Ca	CRESST
Ge	CDMS, EDELWEISS
I	DAMA
Xe	XENON, LUX, PandaX
W	CRESST



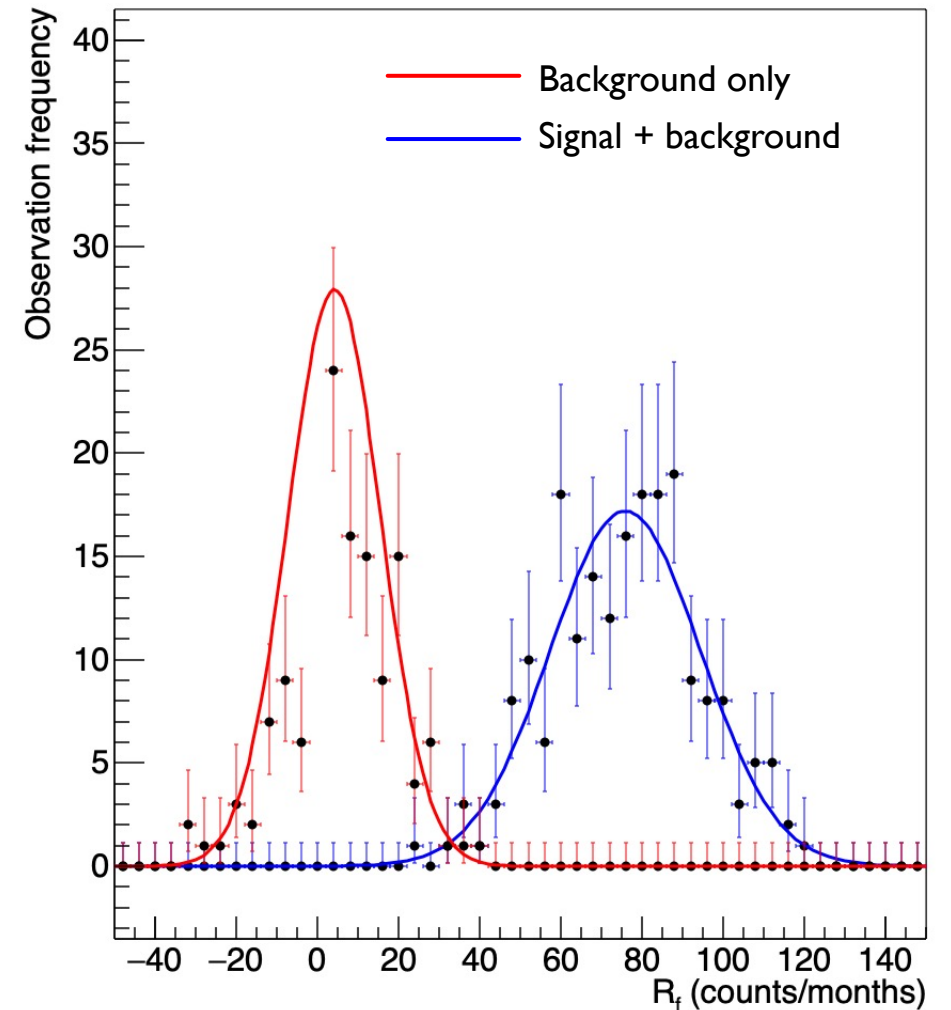
# EVENT RATES

Limits are typically set by assessing how well the signal can be distinguished from detector backgrounds.

Two components to interaction rates with DM used for limit setting:

- Rate of DM interaction with SM
  - Dictated by target, model choice, velocity distribution
- Rate of observation of events
  - Dictated by observation process and detector setup

Can have significantly different energy scales, depending on type of detector.



# INTERACTION RATE

Number of nuclear recoils as a function of nuclear recoil energy  $E_R$

$$\frac{dR}{dE_R} = N_T \frac{\rho}{m_\chi} \frac{\sigma_0 m_T}{2\mu_N^2} \sum_{i,j} \sum_{a,b=0,1} \hat{c}_i^{(a)} \hat{c}_j^{(b)} \left( F_{ij}^{(ab),1}(q) \int \frac{f_{lab}(\vec{v})}{v} d^3v + F_{ij}^{(ab),2}(q) \int v f_{lab}(\vec{v}) d^3v \right).$$

DM and target properties

- Target density
- Target mass
- DM density
- DM mass
- DM cross section

DM interaction model

- Coupling constants
- DM Form factors
- Nuclear response functions

DM velocity distribution



# OBSERVATION RATE

Number of events observed as a function of observation energy  $E_{ee}$  (electron equivalent keV for scintillator detectors)

$$\frac{dR}{dE'} = \epsilon(E') \frac{1}{(2\pi)^{1/2}} \int_0^\infty \frac{dR}{dE_R} \frac{dE_R}{dE_{ee}} \frac{1}{\Delta E_{ee}} \exp \left[ \frac{-(E' - E_{ee})^2}{2(\Delta E_{ee})^2} \right] dE_{ee}$$

The equation is annotated with four colored boxes and arrows pointing to descriptive text:

- Efficiency/threshold** (purple box): Imperfect/realistic detector setup
- Interaction rate** (red box): As per last slide
- Quenching factor** (red box): Transformation from nuclear recoil energy to observable energy
- Resolution** (orange box): Ability to resolve fine details in energy spectrum

# SENSITIVITY COMPUTATION

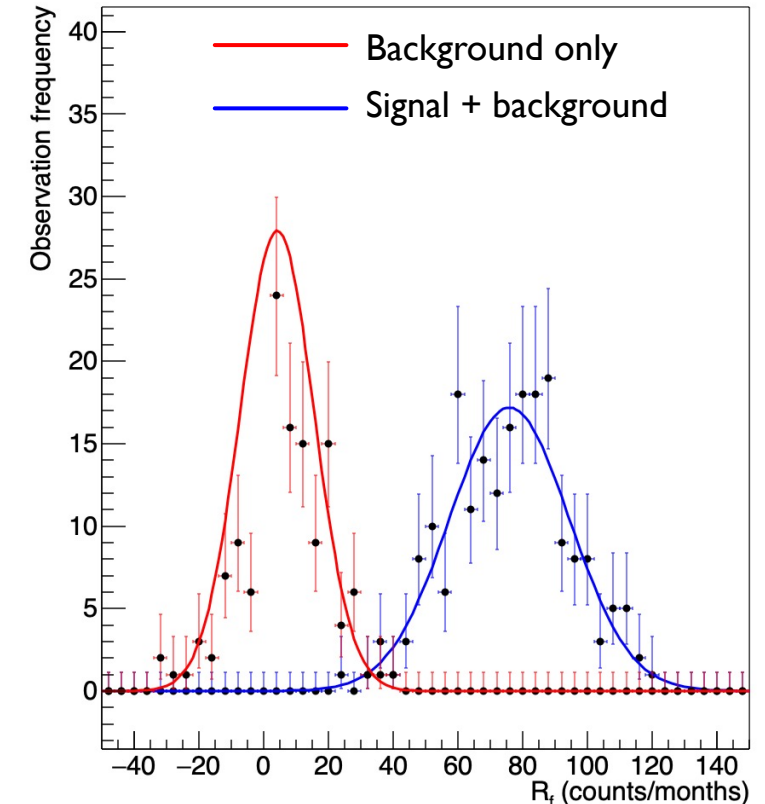
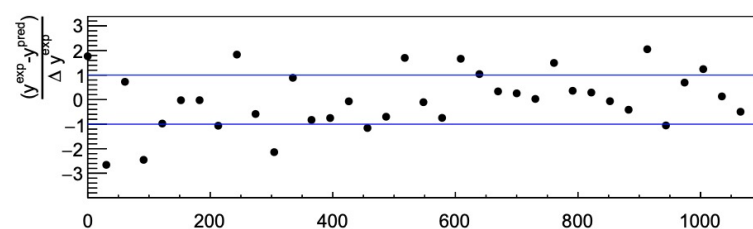
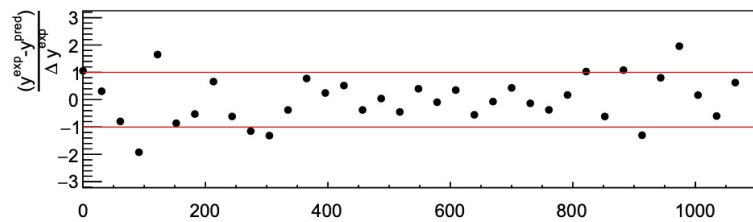
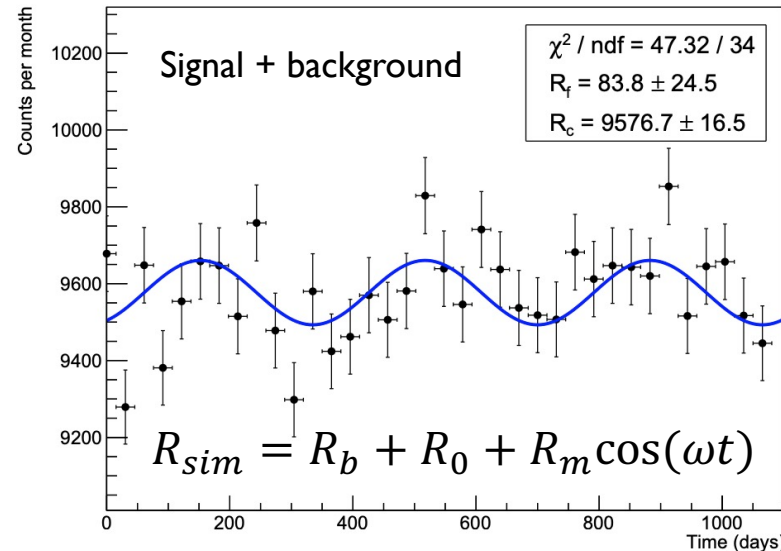
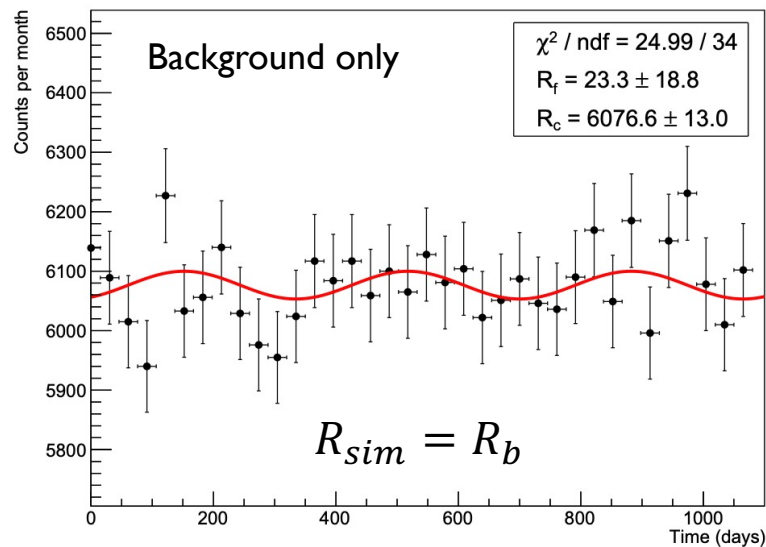
MJZ, Barberio, Busoni JCAP12 (2020) 014

\*we'll come back to the accuracy of this later

DAMA searches explicitly for modulating signal (not constant excess) over a  $\sim$ constant background\*

Need to understand how well statistical fluctuations in a background model mimic modulation.

Simulate this by randomly sampling observed events over detector live time, and fitting to  $R_c + R_f \cos(\omega t)$ .

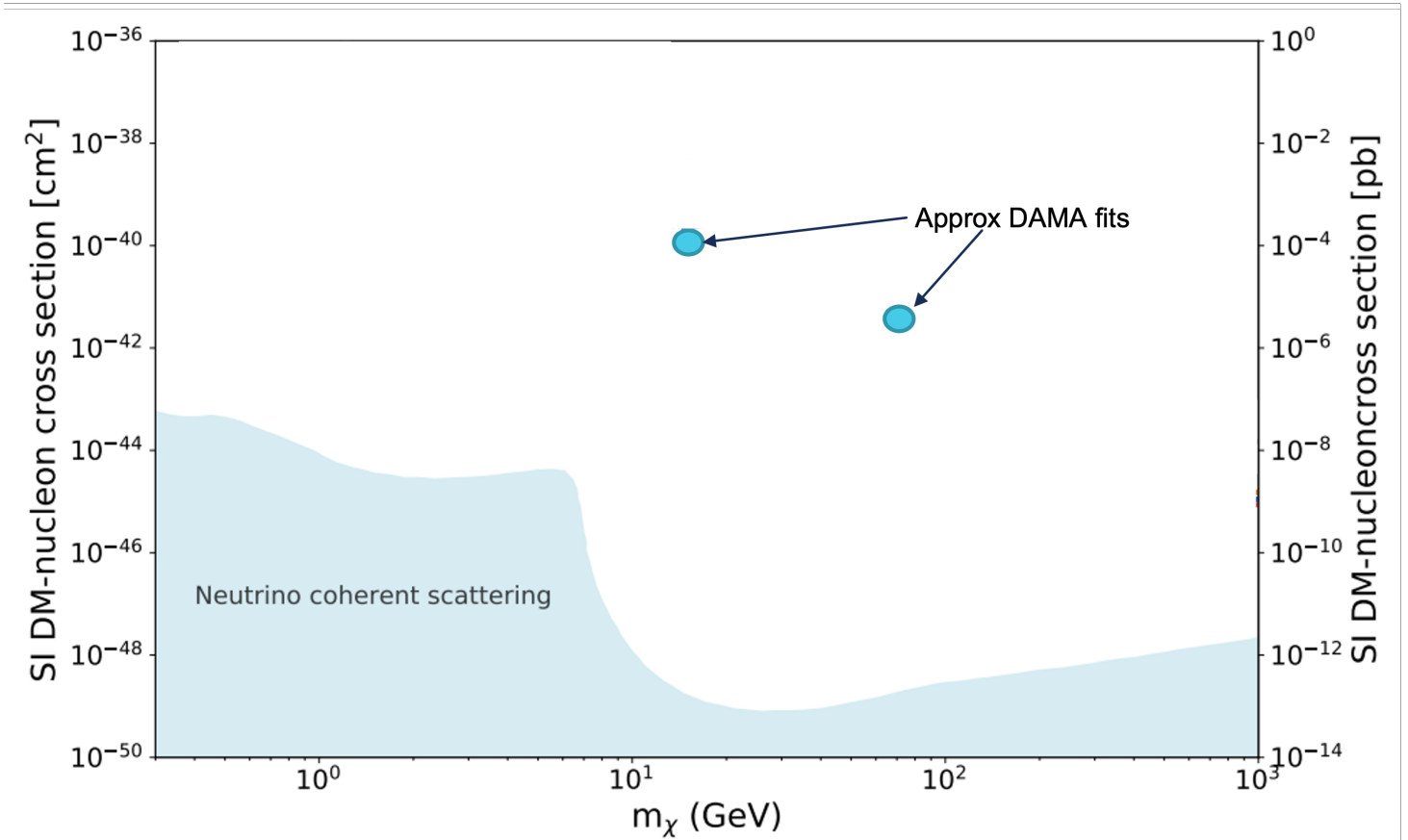


# MODEL DEPENDENCE

[1] Kang, Scopel, Tomar, PRD 99, 103019 (2019)

## Proton-philic inelastic spin dependent WIMP [1]

Target	A	Spin	Experiment/s
<del>O</del>	<del>16</del>	<del>-</del>	<del>CRESST</del>
<del>F</del>	<del>19</del>	<del>p</del>	<del>PICO, PICASSO</del>
<del>Ne</del>	<del>20</del>	<del>-</del>	<del>NEWS-G</del>
<del>Na</del>	<del>23</del>	<del>p</del>	<del>DAMA</del>
<del>Ar</del>	<del>40</del>	<del>-</del>	<del>DEAP, DarkSide</del>
<del>Ca</del>	<del>40</del>	<del>-</del>	<del>CRESST</del>
<del>Ge</del>	<del>73</del>	<del>n</del>	<del>CDMS, EDELWEISS</del>
<del>I</del>	<del>127</del>	<del>p</del>	<del>DAMA</del>
<del>Xe</del>	<del>131</del>	<del>n</del>	<del>XENON, LUX, PandaX</del>
<del>W</del>	<del>184</del>	<del>-</del>	<del>CRESST</del>

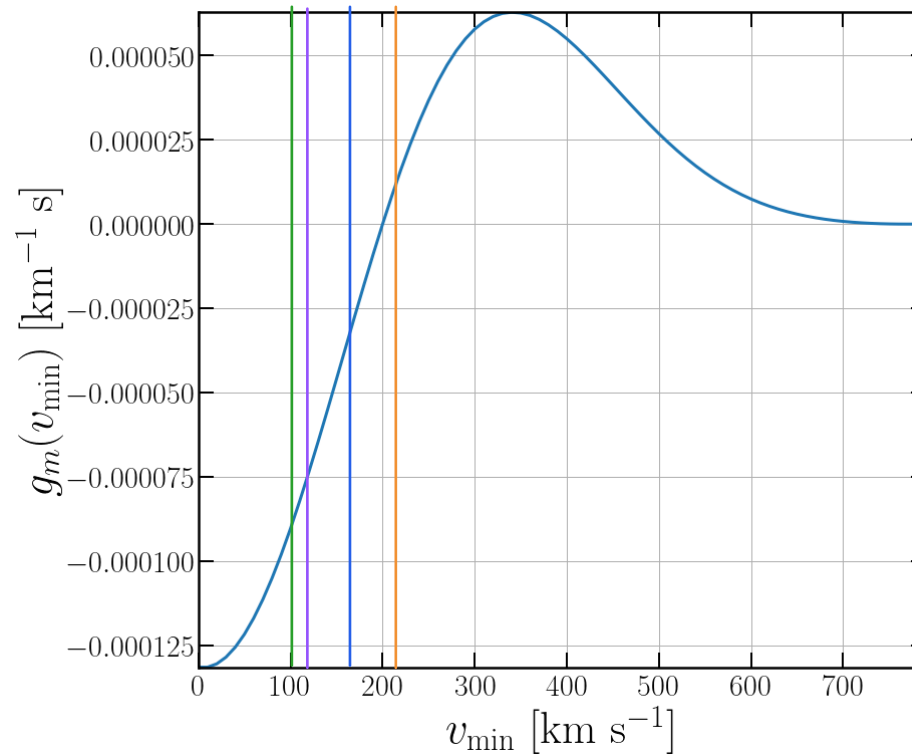
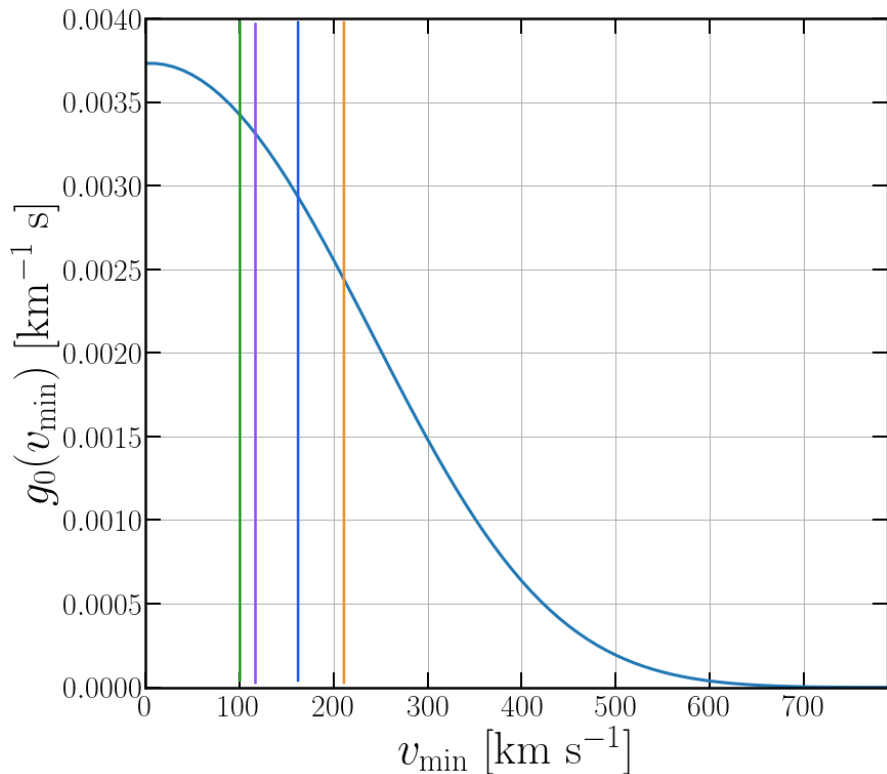


# VELOCITY DISTRIBUTIONS

For chosen velocity distribution useful to express the integral as a function of minimum velocity – depends on target and DM mass. Expected modulation will be different for different targets.

Positive modulation for one target  $\neq$  Positive modulation at another

$$g(v_{\min}) = \int_{v_{\min}}^{v_{\text{esc}}} v f_{\text{lab}}(\vec{v}) dv d\Omega \quad h(v_{\min}) = \int_{v_{\min}}^{v_{\text{esc}}} v^3 f_{\text{lab}}(\vec{v}) dv d\Omega \quad v_{\min} = \sqrt{\frac{m_T E_R (m_\chi + m_T)^2}{2m_\chi^2 m_T^2}}$$



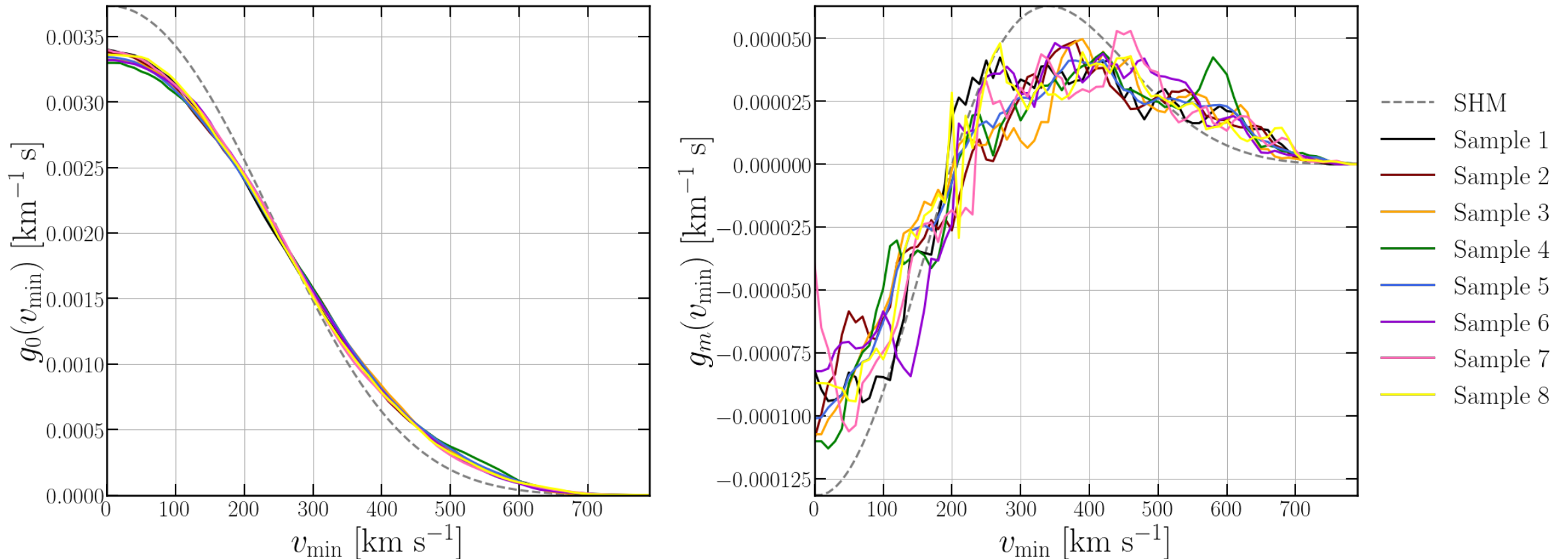
For  $m_\chi = 70 \text{ GeV}/c^2$ :

Target	$v_{\min}$
Ge	101 km/s
Xe	117 km/s
I	174 km/s
Na	207 km/s

# VELOCITY DISTRIBUTIONS

[1] Lawrence et al., arxiv:2207.07644

Realistic galaxy simulations [1] suggest the presence of substructure that influences the expected modulation



# REQUIREMENTS FOR MODEL INDEPENDENCE

Such a large collection of model possibilities, need to assess using the same target and as similar a set up as possible

$$\frac{dR}{dE'} = \epsilon(E') \frac{1}{(2\pi)^{1/2}} \int_0^\infty \frac{dR}{dE_R} \frac{dE_R}{dE_{ee}} \frac{1}{\Delta E_{ee}} \exp \left[ \frac{-(E' - E_{ee})^2}{2(\Delta E_{ee})^2} \right] dE_{ee}$$

**Interaction rate** the same for all NaI detectors. No need to choose a model, just perform Boolean check.

Test for a modulation that has the same ratio of  $R_m/R_0$  as DAMA (exact value may change based on set up)

Cannot construct a true model independent test from constant constraints alone

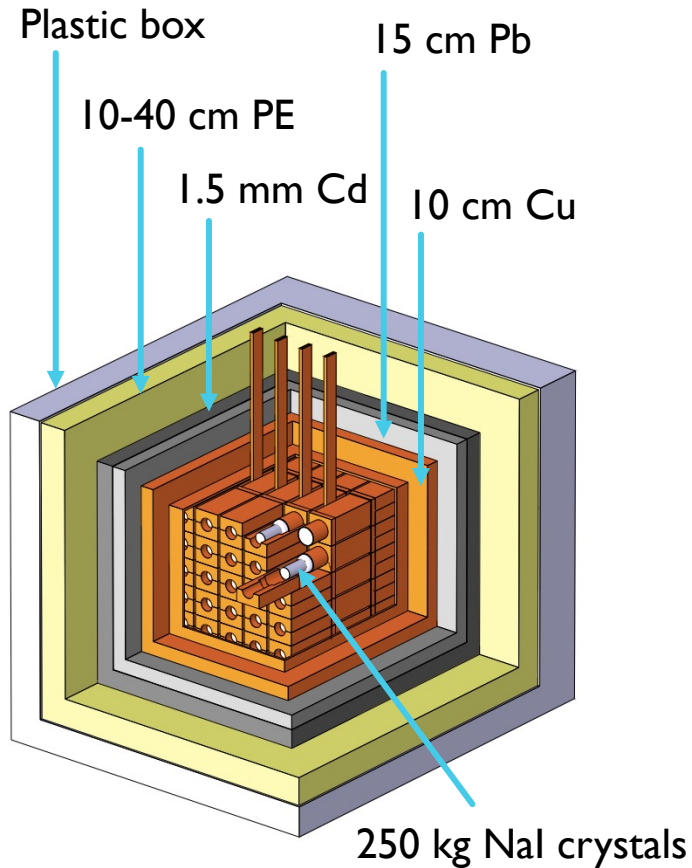
Need to assume a model to map DAMA modulation onto constrained parameter space

# NAI DETECTORS

[1] Bernabei et al. PPNP 114 103810 (2020)  
[2] Adhikari et al. EPJC 78, 107 (2018)  
[3] Amare et al. PRD 103, 102005 (2021)

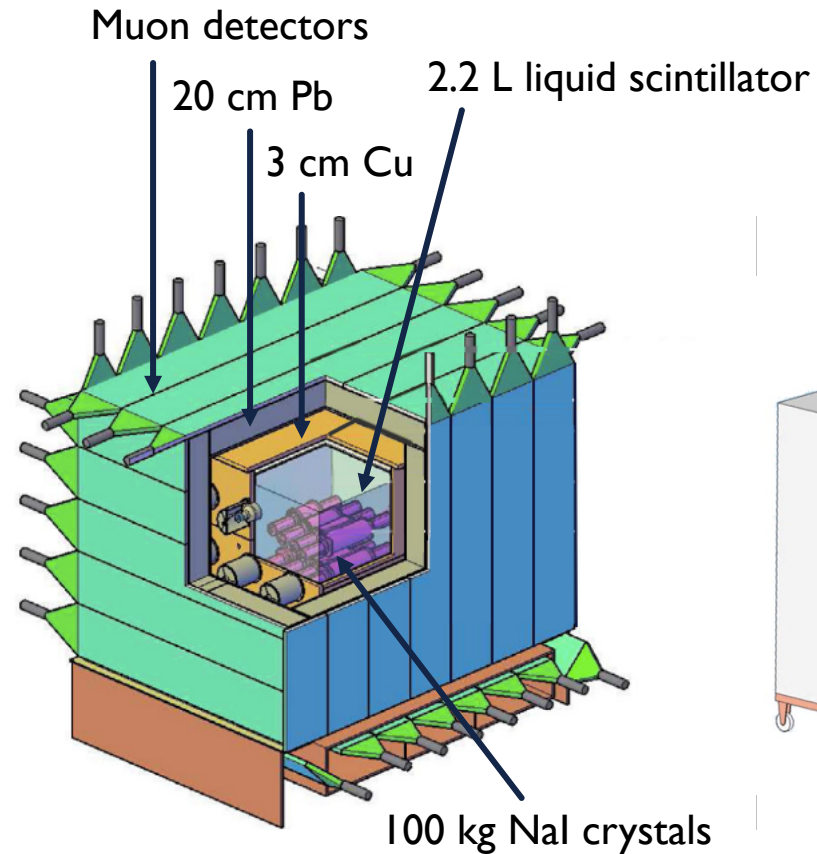
## DAMA<sup>[1]</sup>

Background  $\sim 0.8$  cpd/kg/keV



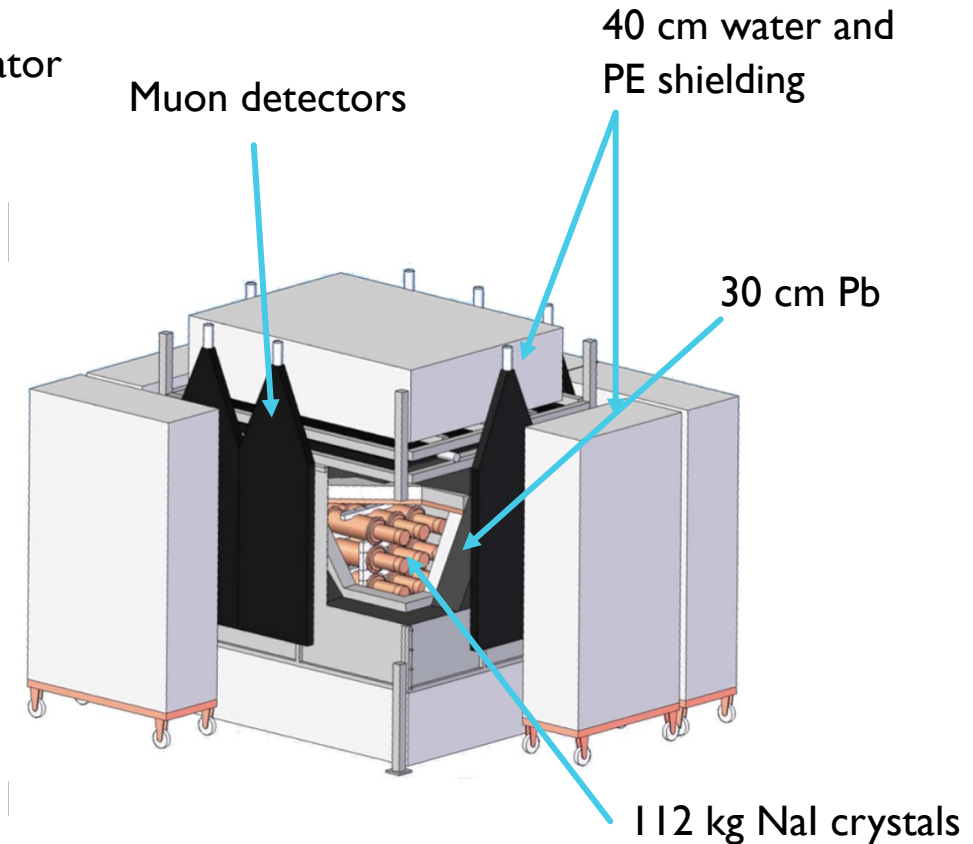
## COSINE<sup>[2]</sup>

Background  $\sim 2.9$  cpd/kg/keV



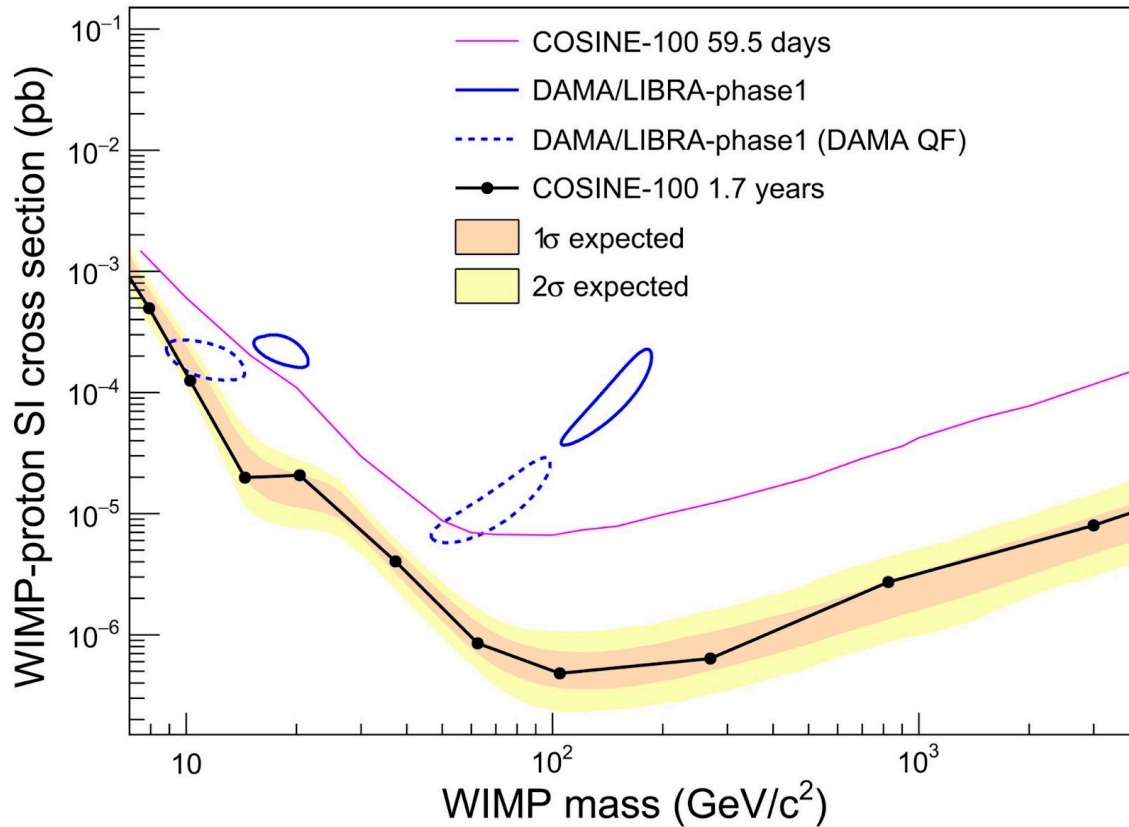
## ANAIS<sup>[3]</sup>

Background  $\sim 3.2$  cpd/kg/keV

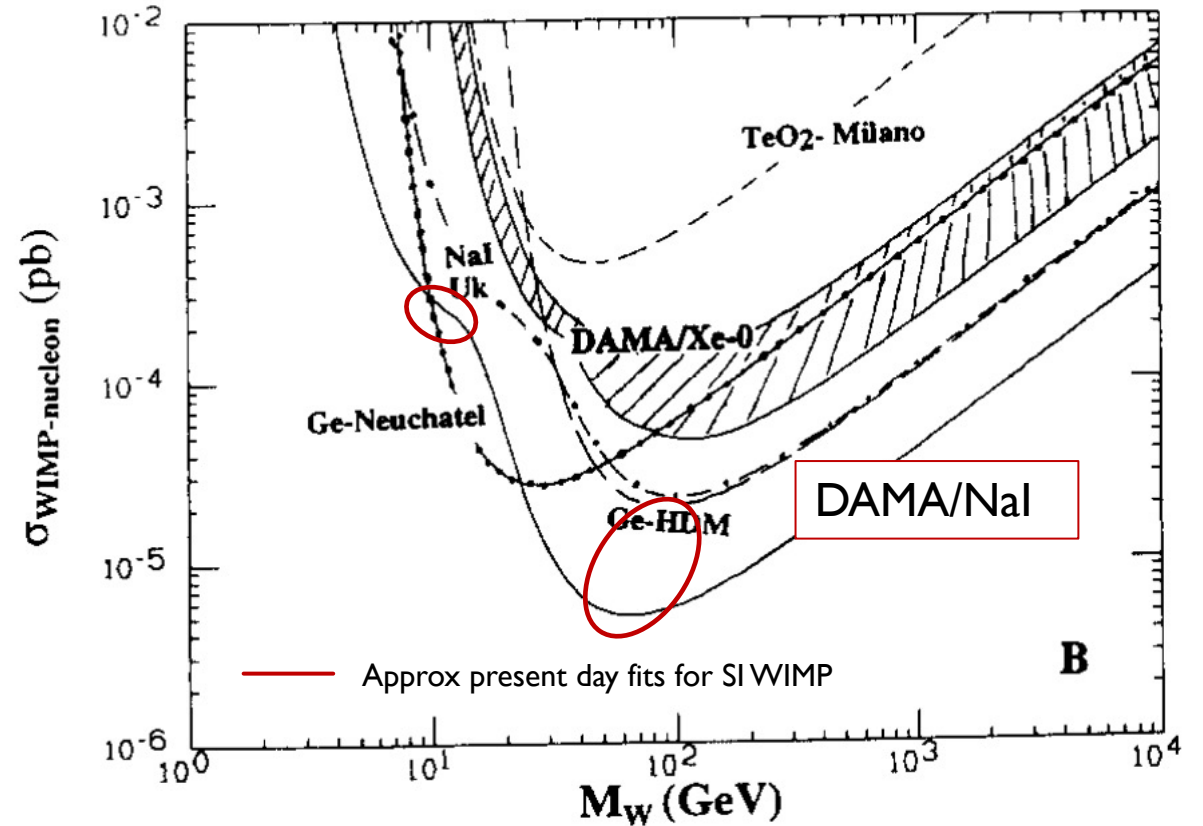


# RECENT RESULTS

Most “damning” NaI constraints to date are based on lack of constant excess  $\Rightarrow$  model dependent test  
 But! This region already strongly constrained by DAMA from its first data taking.



Adhikari et al. (COSINE Collaboration) [10.1126/sciadv.abk2699](https://doi.org/10.1126/sciadv.abk2699)



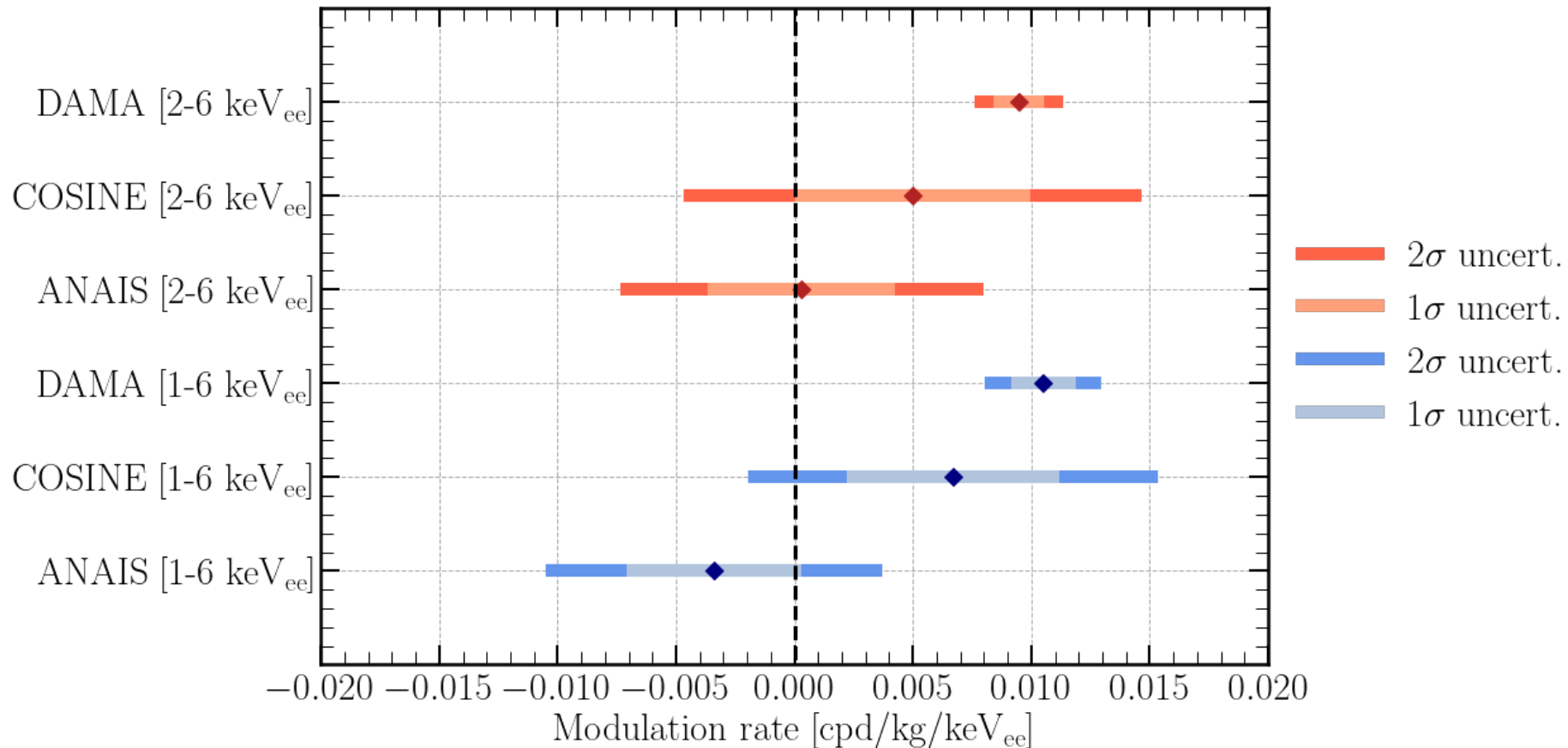
Bernabei et al. (DAMA Collaboration) [10.1016/S0370-2693\(96\)80020-7](https://doi.org/10.1016/S0370-2693(96)80020-7)



# RECENT RESULTS

[1] Bernabei et al. PPNP 114 103810 (2020)  
[2] Adhikari et al. arxiv:2111.08863  
[3] Amare et al. PRD 103, 102005 (2021)

For modulation searches, both COSINE and ANAIS are beginning to reach strong sensitivity, but at present both still compatible with DAMA and null hypothesis within  $3\sigma$  due to high backgrounds



# DETECTOR DEPENDENCIES

Difficulty with model independent tests is then slight differences between detector setups.  
Need to understand if these can introduce 'hidden' model dependence – i.e., will these changes appear more extreme for different models/masses of DM?

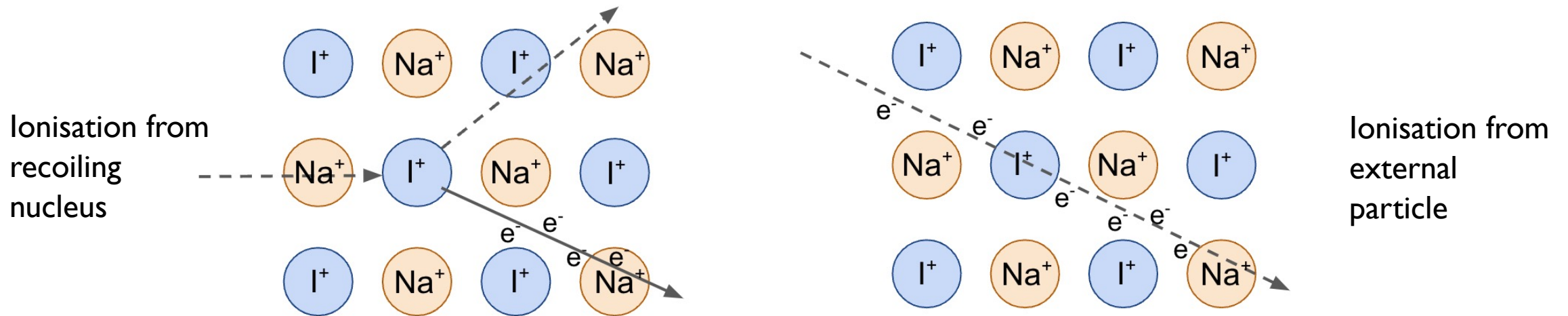
Potential differences of interest:

- Na quenching factor
  - Radioactive backgrounds
  - Electronic backgrounds
  - Background modelling
  - Location specifics
  - Energy thresholds
- Background modelling and mitigation

# QUENCHING FACTOR

Purpose is to convert nuclear recoil energy (signal) into electron equivalent energy (used to calibrate the detector).

$$E_{ee} = Q(E_{NR})E_{NR}$$



Possible that this effect depends strongly on optical properties of crystals so different growth methods can impact results. Interesting to think about as:

- Differences observed in QF measurements by different groups
- Would change both amplitude and position of signal
- Depends on the nucleus DM interacts with so impacts different masses in different ways

# QUENCHING FACTOR MEASUREMENTS

Why are the DAMA quenching factors different to those measured since?

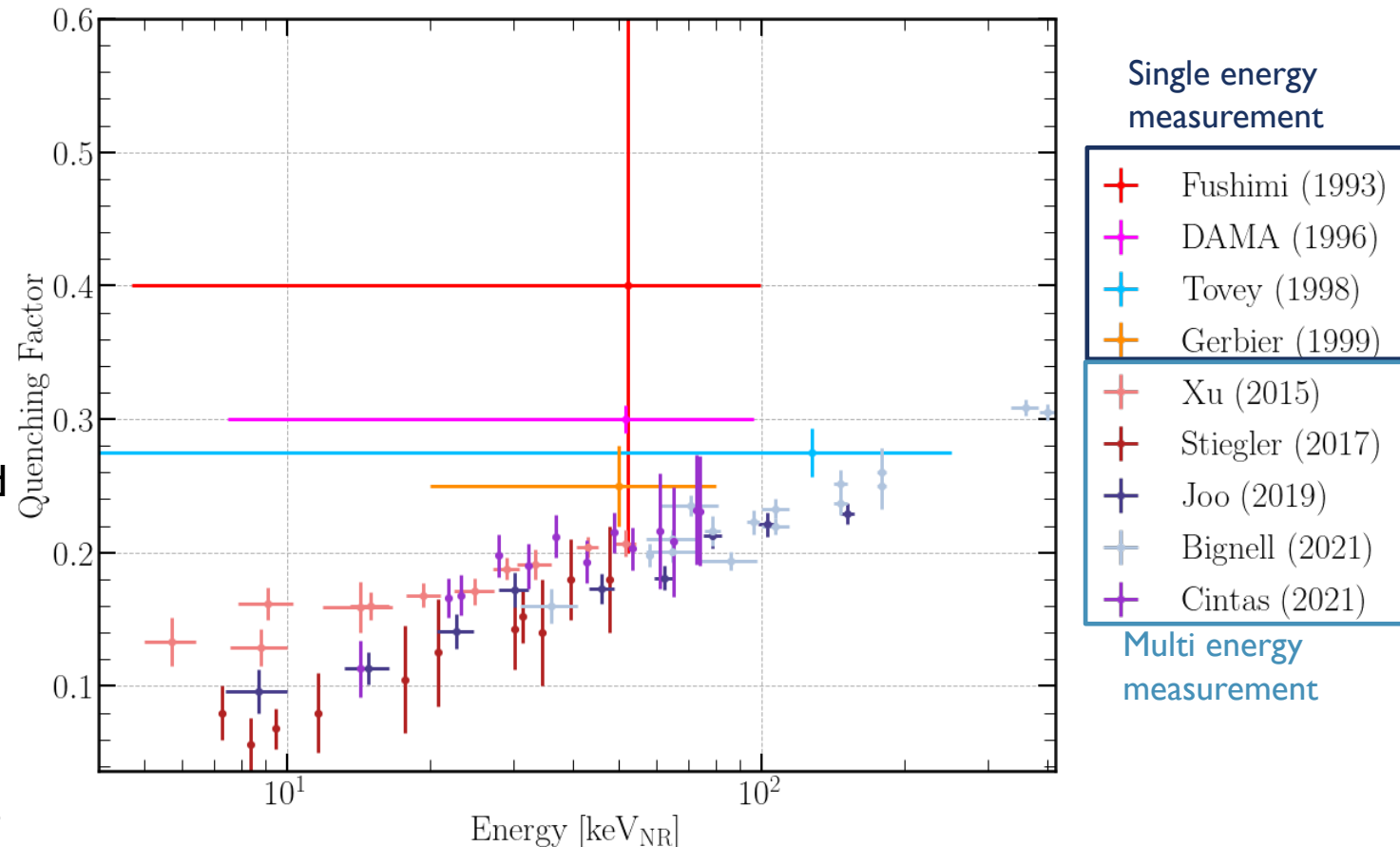
Possible solutions:

1. Differences in measurement method
2. QF is something that changes crystal to crystal

Particular solution will influence how data should be interpreted and compared.

Possible that (1) and (2) are both true - still inconsistencies at low energy.

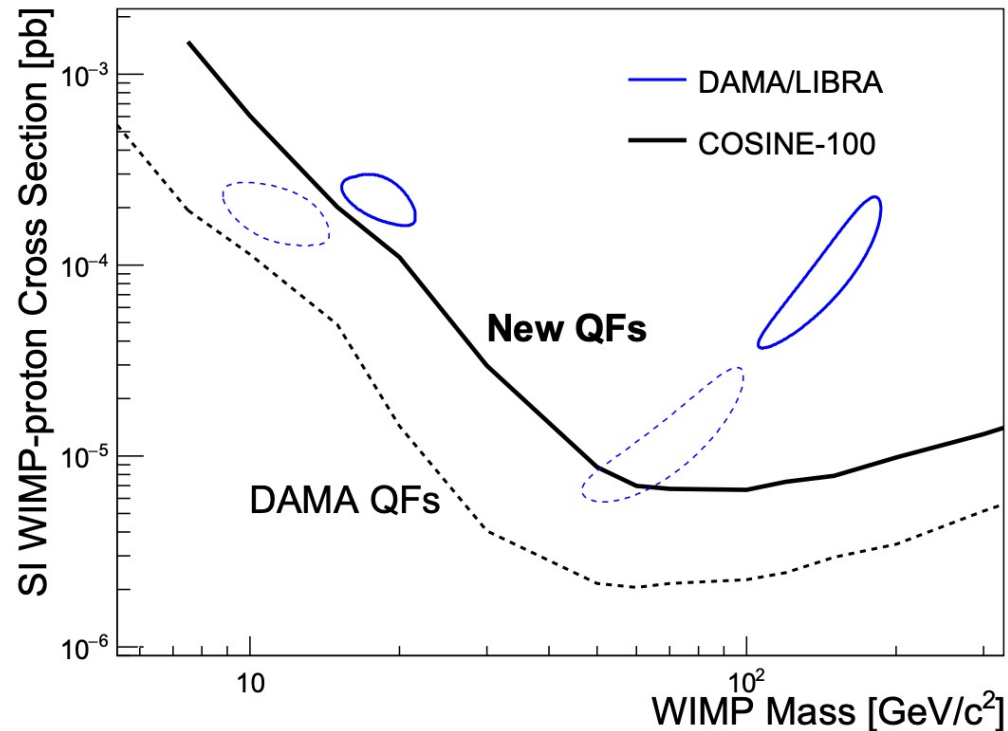
Also the question of energy dependence – is this a feature of calibration? (See Cintas et al.)



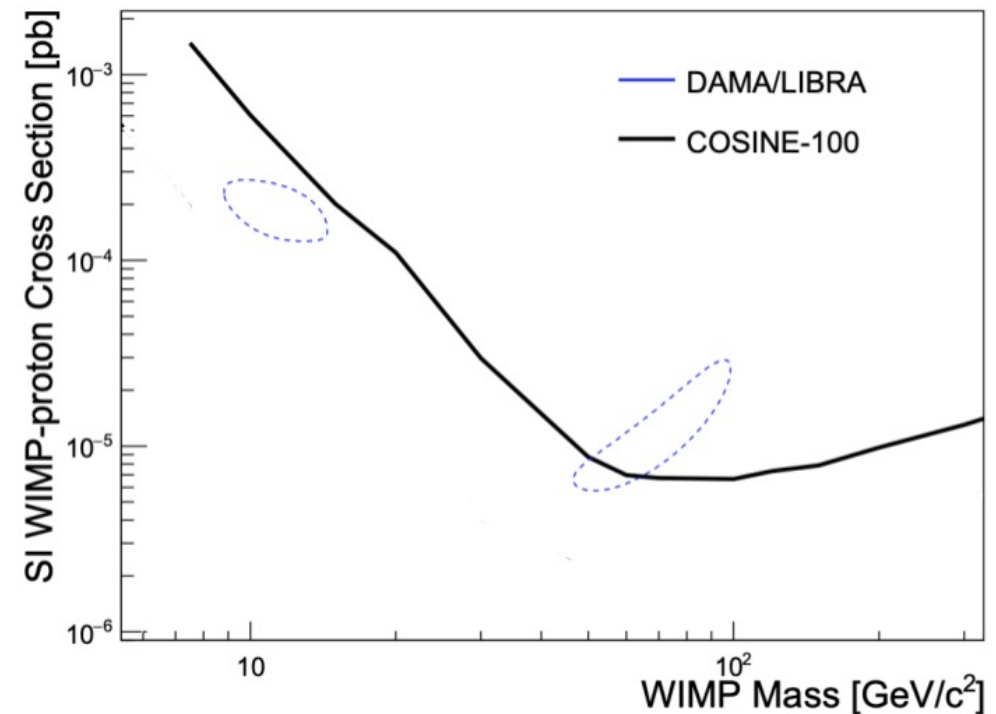
# QUENCHING FACTOR IMPACT

[1] Adhikari et al. *JCAP* 11 (2019)

Can use results presented by COSINE [1] to understand how different QF combinations impact exclusion of DAMA



Assuming detectors have the same QF (either the solid or dotted lines)



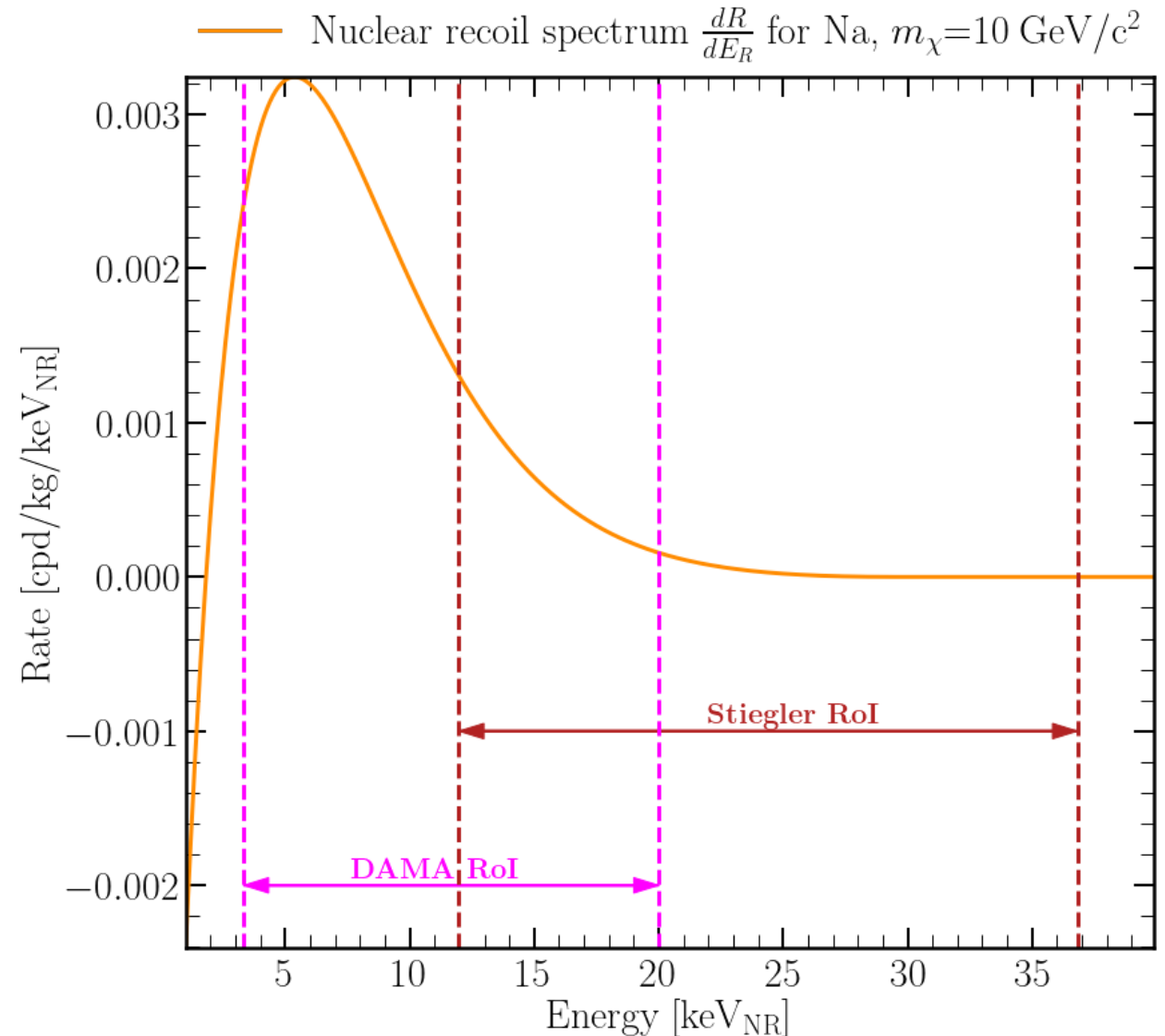
Assuming detectors have different QFs

# QUENCHING FACTOR IMPACT

Change of QF has a strong influence on the observable rate.

Changing relationship between NR and observed energy means the 1-6 keV<sub>ee</sub> observable region of interest is “accessing” different parts of the nuclear recoil energy spectrum.

This will impact all DM interaction models, where the extent of the impact is dictated by the shape of the recoil spectrum

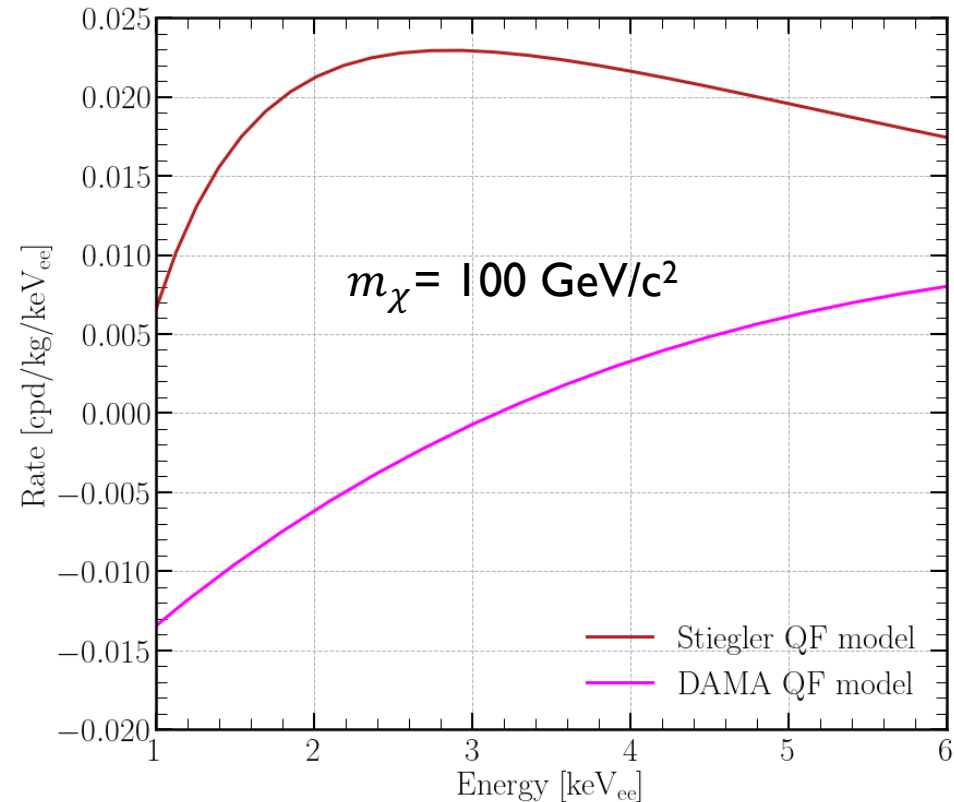
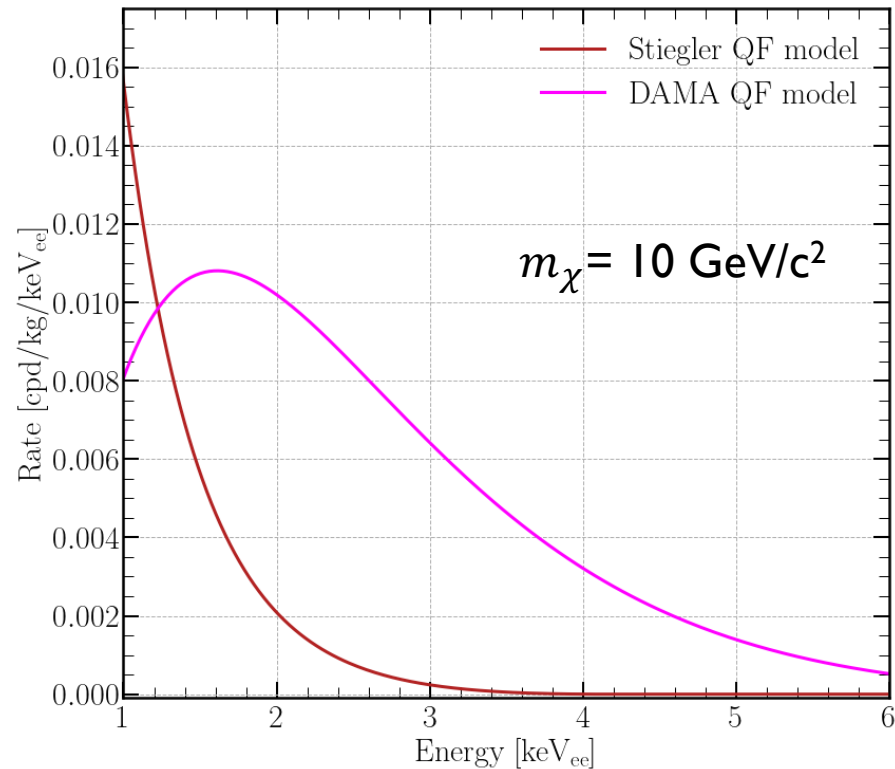


# QUENCHING FACTOR IMPACT

R. Bernabei et al. Riv Nuovo Cim 26 (2003)  
T. Stiegler et al. 2017 arxiv:1706.07494

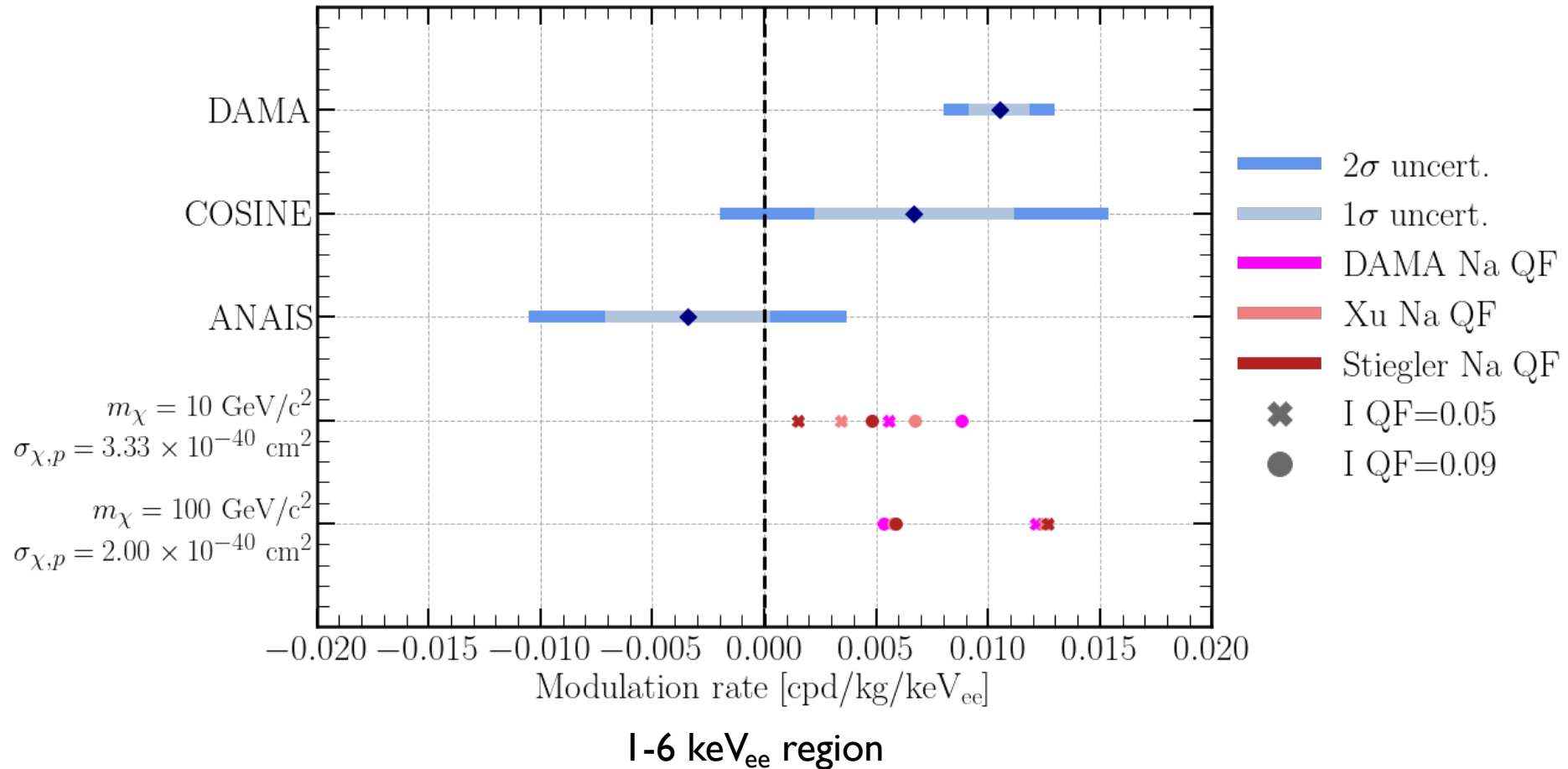
Detector differences can still change the observed modulation even if the interaction rate is the same  
e.g., for low mass spin independent DM,  $m_\chi = 10 \text{ GeV}/c^2$ , a change to the QF drastically changes the observable signal, both in value and shape in the region of interest. Effect is more pronounced than for  $m_\chi = 100 \text{ GeV}/c^2$

⇒ Even for tests with the same target, no guarantee the modulation will look the same



# QUENCHING FACTOR IMPACT

This toy model w/ different QFs can produce modulation amplitudes more consistent with other observations  
 Effect is strongly dependent on DM model and mass  $\Rightarrow$  model independent test is impossible



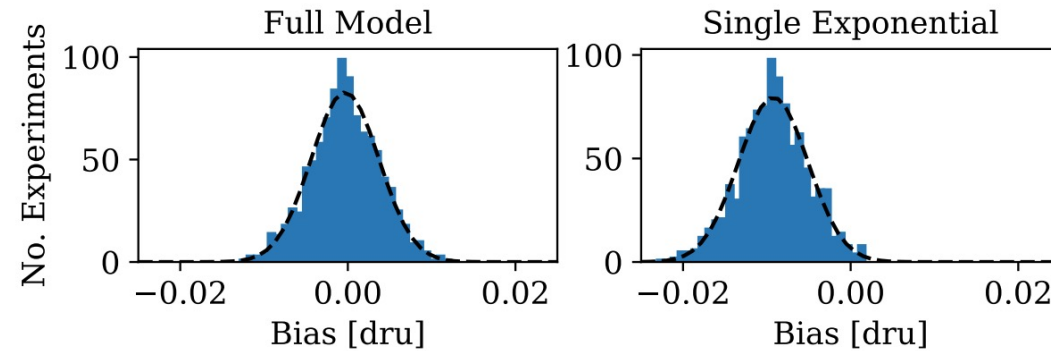


# BACKGROUND MODELS

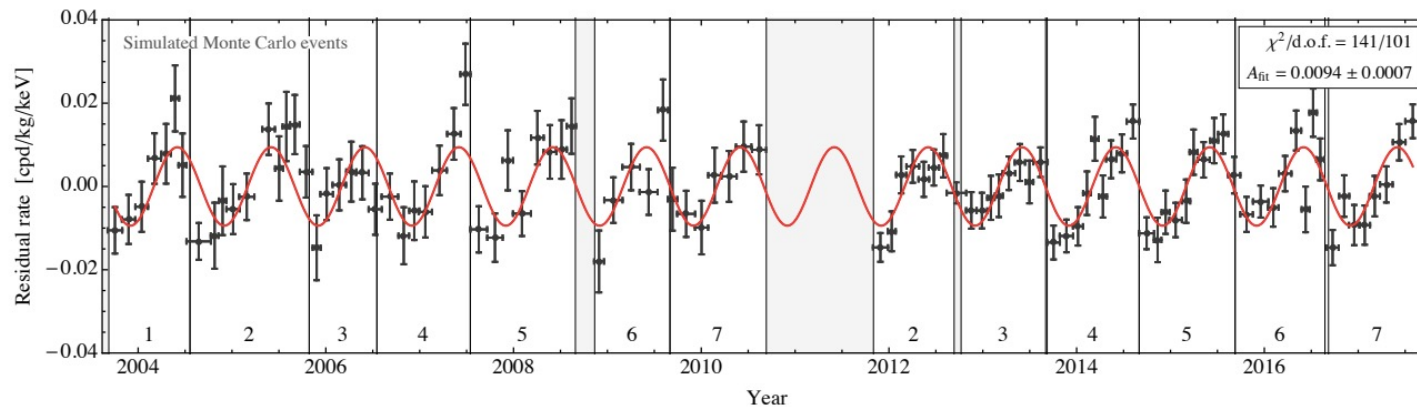
[1] Adhikari et al. arxiv:2111.08863  
[2] Buttazzo et al JHEP04(2020)137

COSINE and Buttazzo et al. demonstrated influence of improperly modelled backgrounds:

1. Introduction of bias from simplistic time dependence [1]



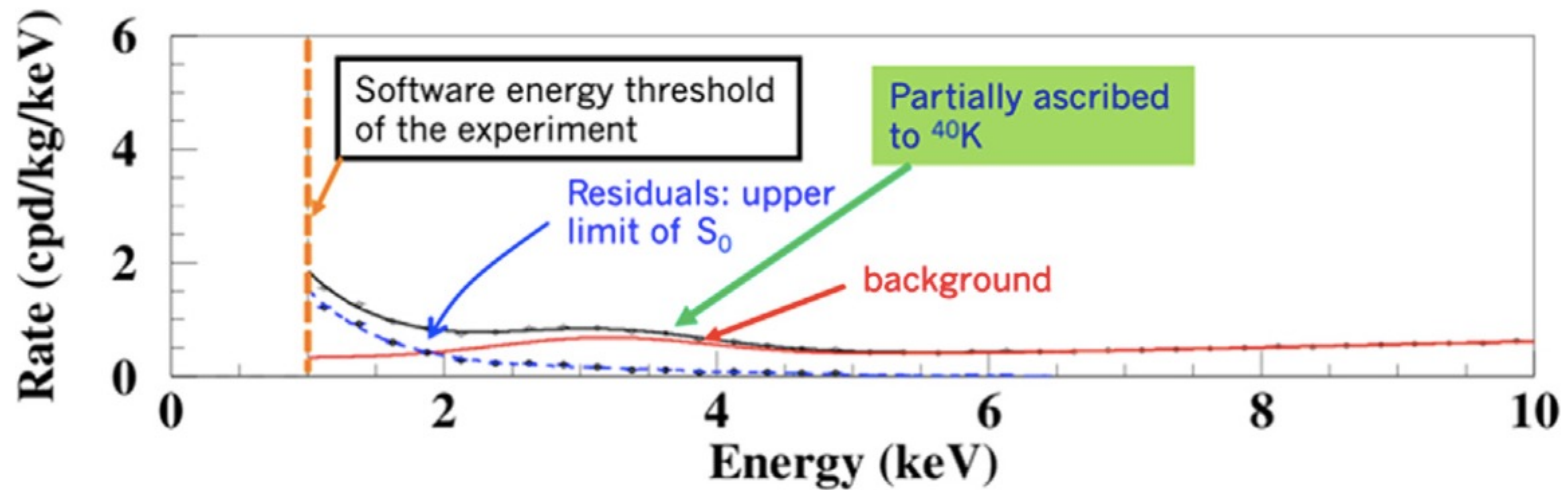
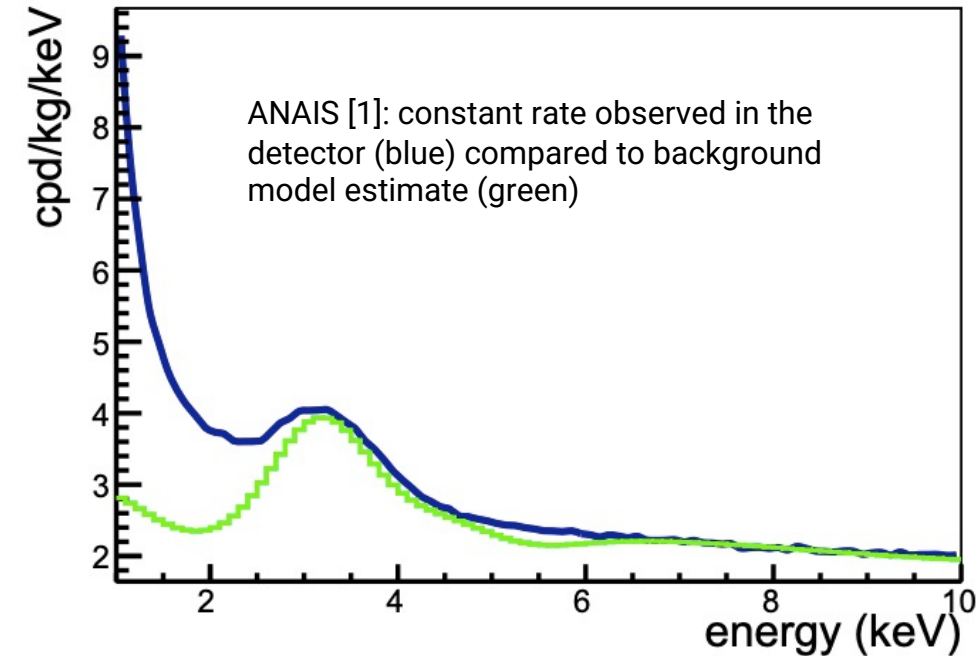
2. Introduction of modulation from assumption of constant background in time and subtracting the averaged rate [2]



# BACKGROUND MODELS

[1] Amare et al. Phys. Rev. D 103, 102005 (2021)  
[2] Bernabei et al. PPNPI 14 103810 (2020)

Clear that background modelling is difficult especially in the low energy region due to PMT noise etc.



⇒ need a low background, well modelled experiment to understand if modulation is real or an artifact of analysis

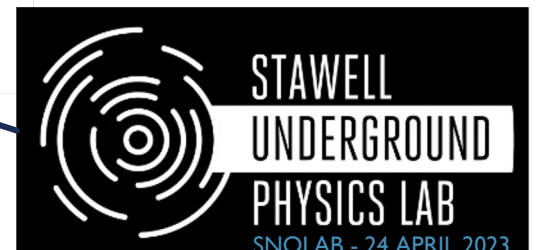
# THE SABRE COLLABORATION

Experimental program to test the DAMA modulation based around detectors place in two different locations:

- SABRE North at Laboratori Nazionali del Gran Sasso (LNGS) in Italy
- SABRE South at Stawell Underground Physics Laboratory (SUPL) in Australia



Istituto Nazionale di Fisica Nucleare  
Laboratori Nazionali del Gran Sasso



# THE SABRE COLLABORATION

SABRE North and South detectors have **common core features**, both employing:

- Same detector module concept (Ultra-pure crystals and HPK R11065 PMTs)
- Common simulation, DAQ and software frameworks
- Exchange of engineering know-how with official collaboration agreements between the ARC Centre of Excellence for Dark Matter and the INFN

SABRE North and South detectors **have different shielding designs**:

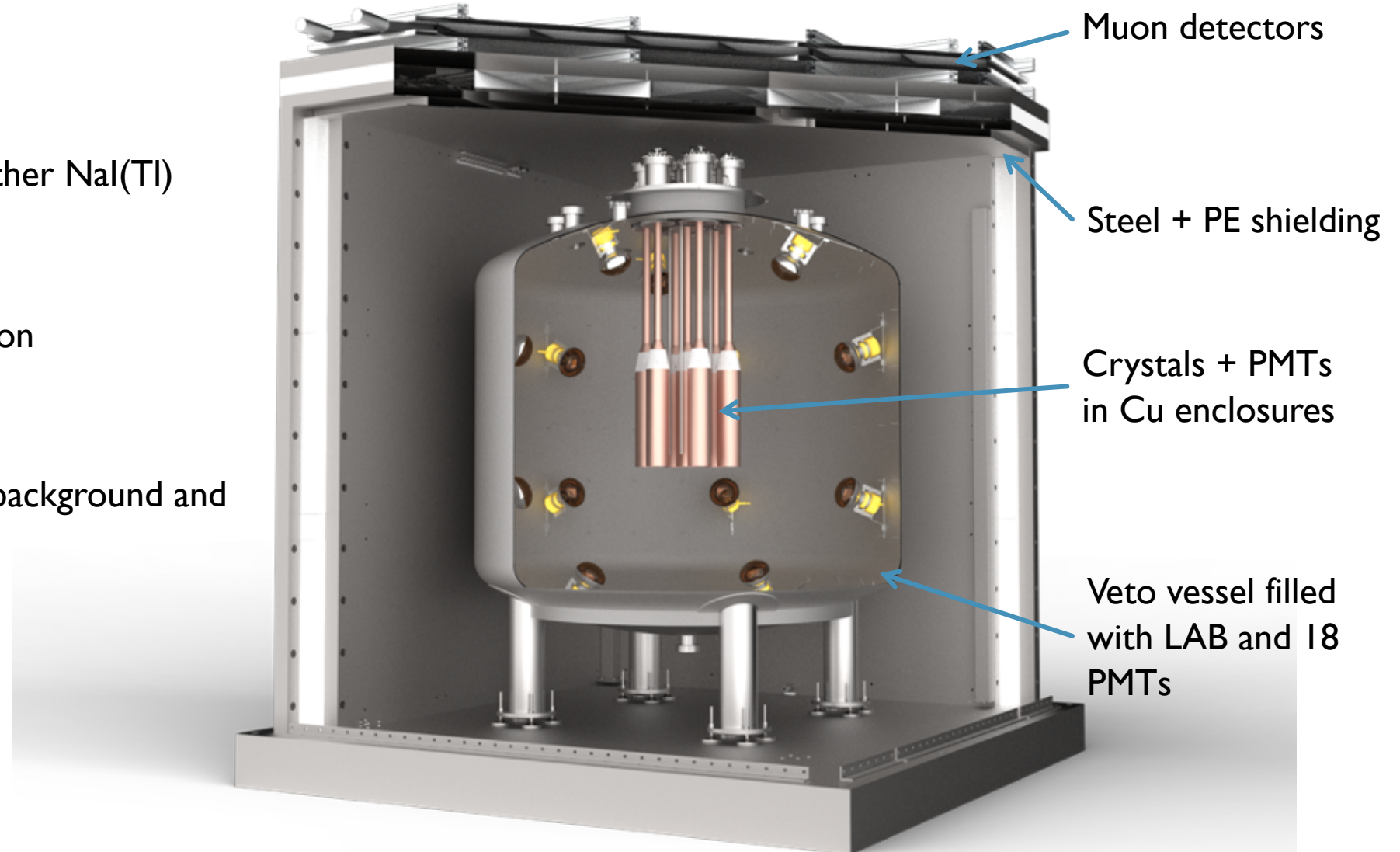
- SABRE North has opted for a fully passive shielding due to the phase out of organic scintillators at LNGS. Direct counting and simulations demonstrate that this is compliant with the background goal of SABRE North at LNGS.
- SABRE South will be the first experiment in SUPL, the liquid scintillator will be used for in-situ evaluation and validation of the background in addition of background rejection and particle identification.

# SABRE

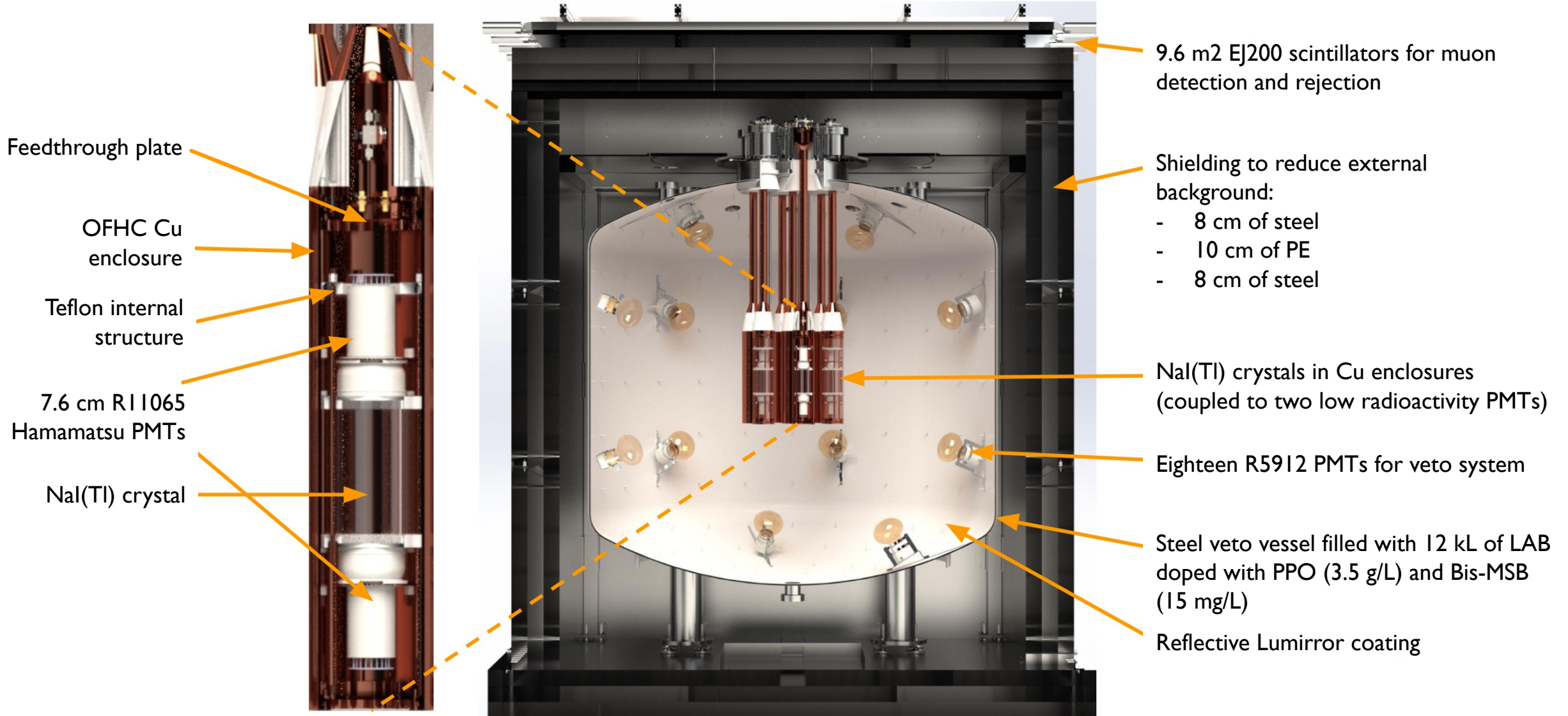
Four key improvements on other NaI(Tl) detectors:

1. Ultra-high purity crystals
2. Active background rejection
3. Low energy threshold
4. Dual hemisphere data

Will provide unprecedented background and sensitivity



# SABRE SOUTH



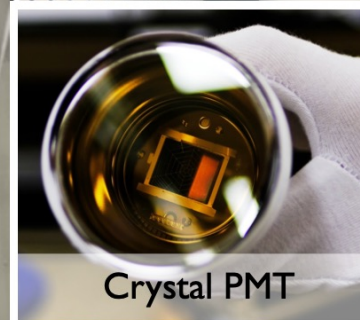
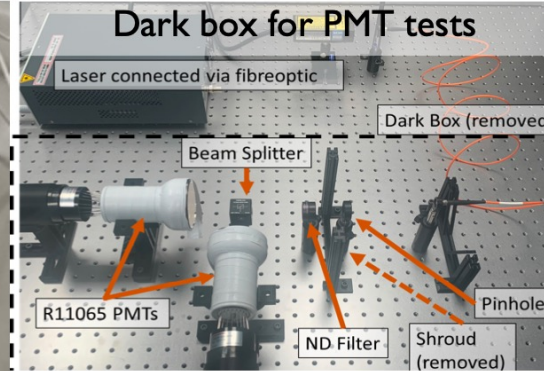
# SABRE SOUTH



SABRE South vessel, Madeleine for scale



SABRE South crystal currently being characterized at LNGS



Crystal PMT



Veto PMT



LAB from JUNO ready for SUPL

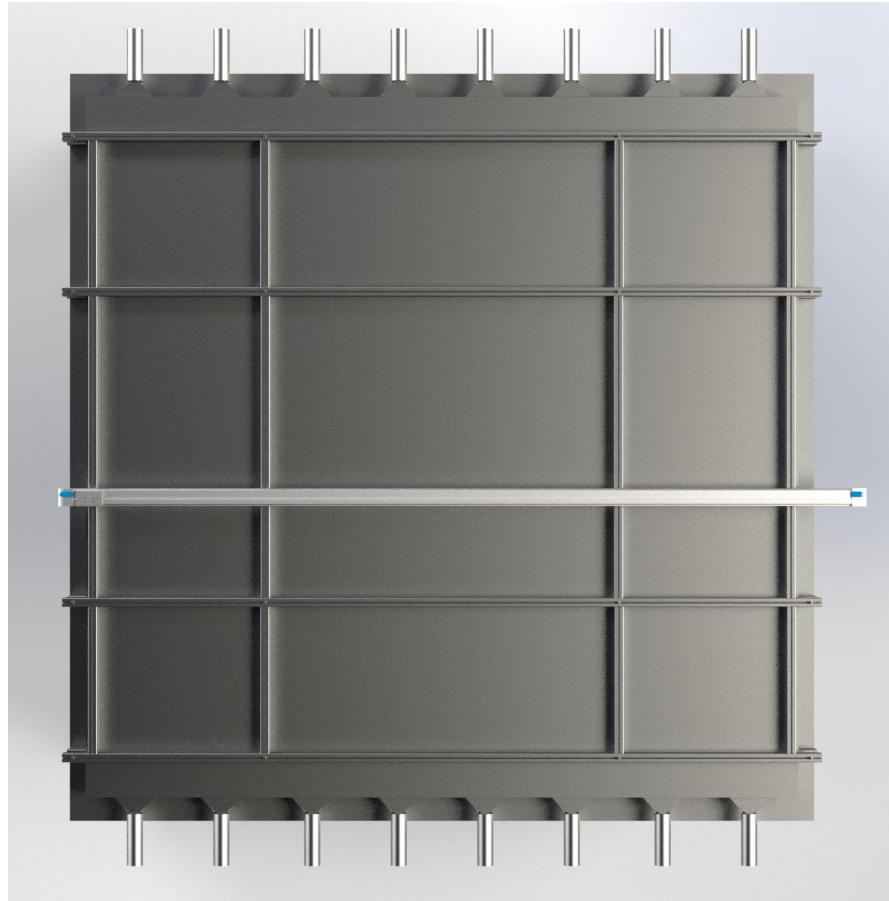
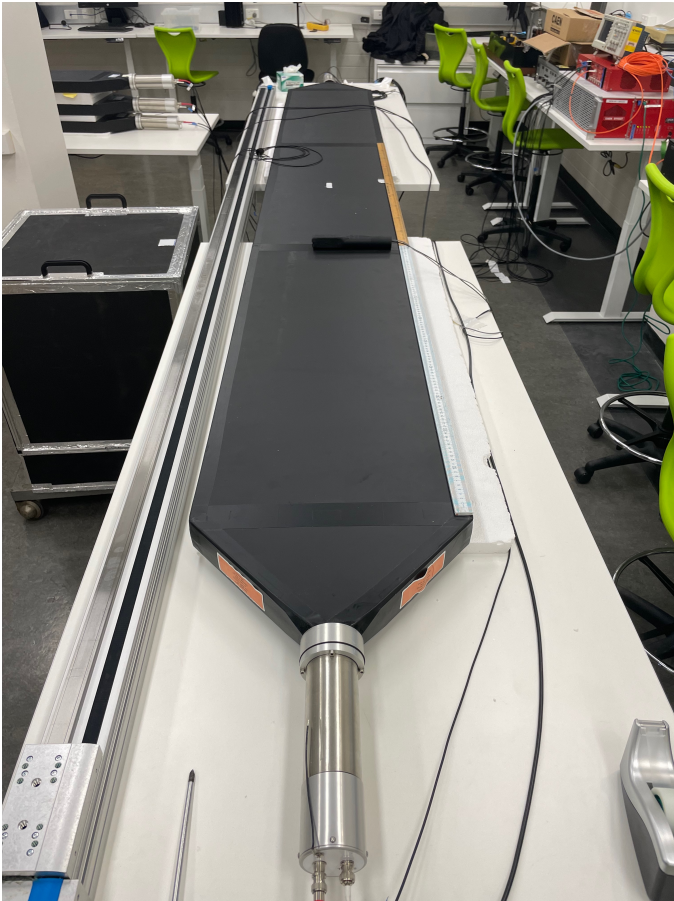


Crystal enclosure + conduit



Muon detector

# MUON DETECTOR SYSTEM



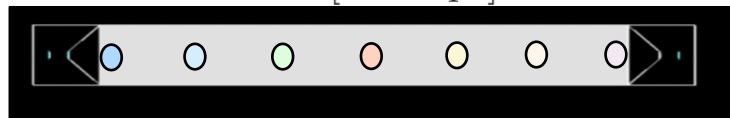
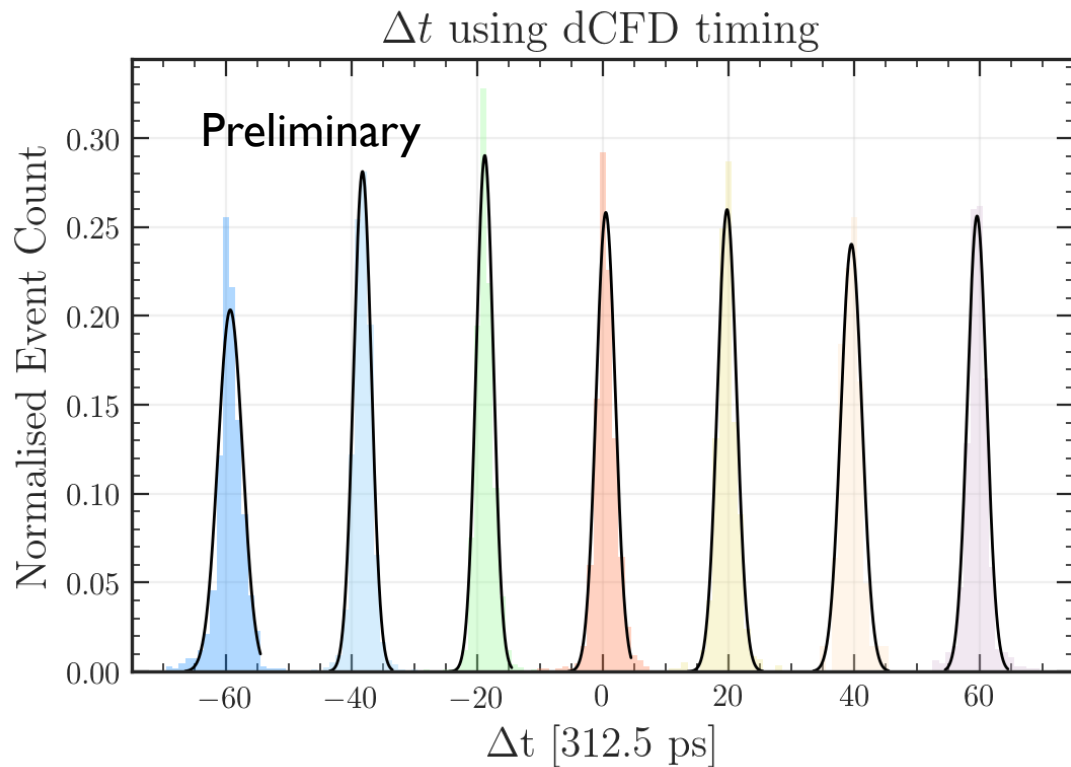
Muon detection system:

- Eight 3 m long EJ200 detector paddles
- Total coverage  $9.6 \text{ m}^2$  above main vessel
- Each coupled to two R13089 PMTs and sampled at 3.2 GS/s.
- Calibrated with Festo system, threshold on the MeV scale

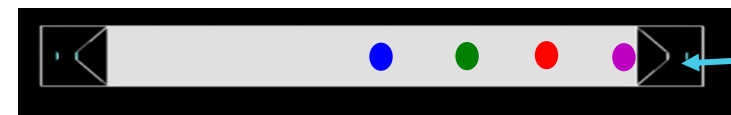
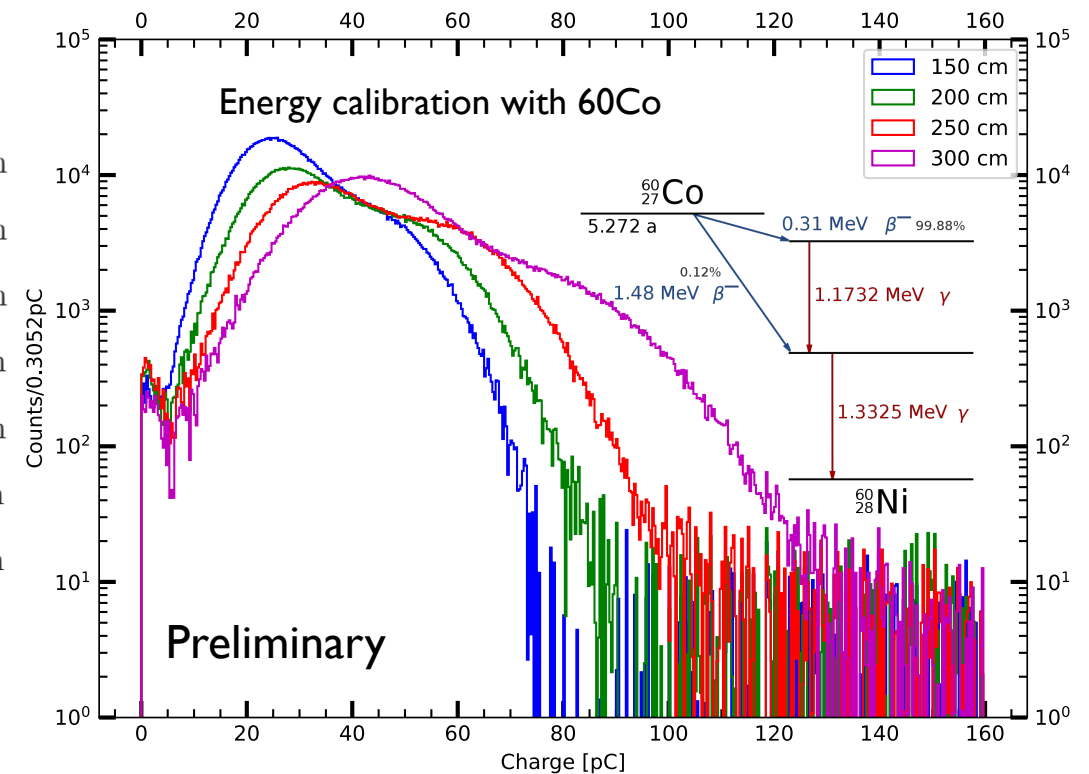


# MUON DETECTOR SYSTEM

Detectors have 400 ps timing resolution, giving a 5 cm position resolution. Characterisation is ongoing underground. This allows for long term measurement of the muon flux, and particle ID when used with the liquid veto system.



Position of source



Position of source

PMT recording charge

# ACTIVE VETO SYSTEM

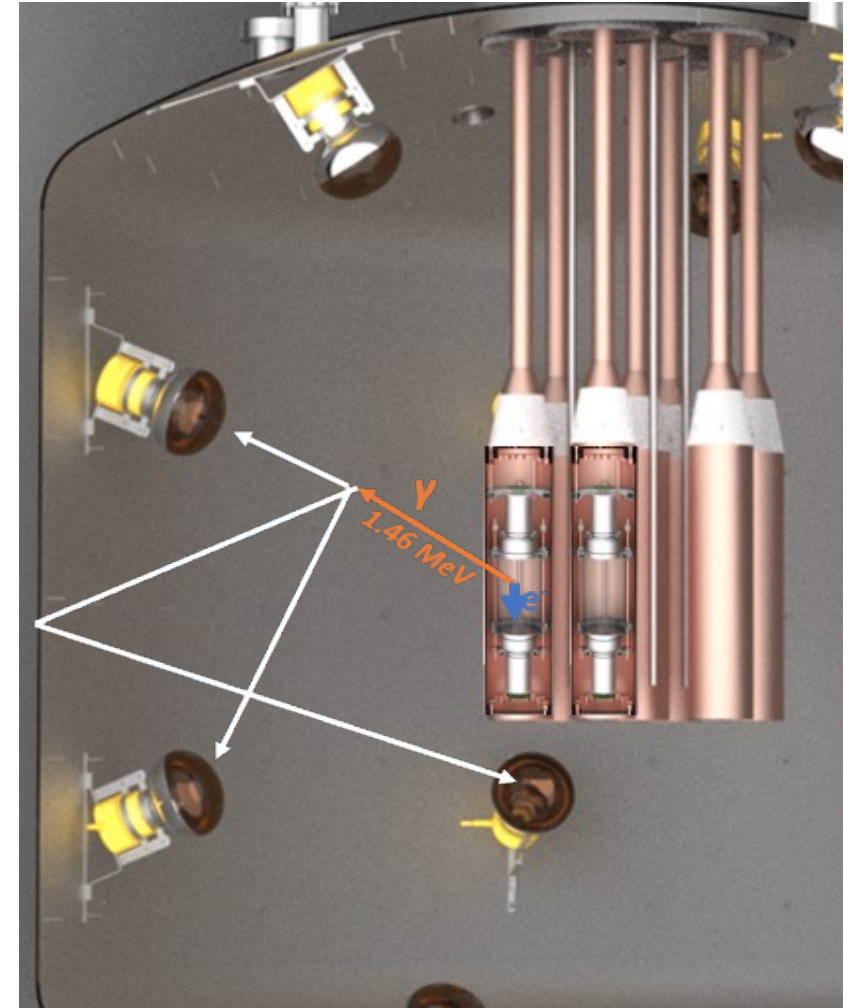
SABRE also utilizes an external tagging system that identifies and reduces background during operation.

System has  $4\pi$  coverage made up of:

- 12 kL linear alkyl benzene doped with PPO and Bis-MSB
- 18 Hamamatsu R5912 PMTs

Any radioactive decay with gamma  $> 100$  keV can be vetoed.  
Average light yield of  $\sim 0.12$  PE/keV, though strong position dependence.

With a threshold of 50 keV it is able to reduce the background by 25%, giving a total background of  $< 1$  cpd/kg/keV.



# ACTIVE VETO SYSTEM

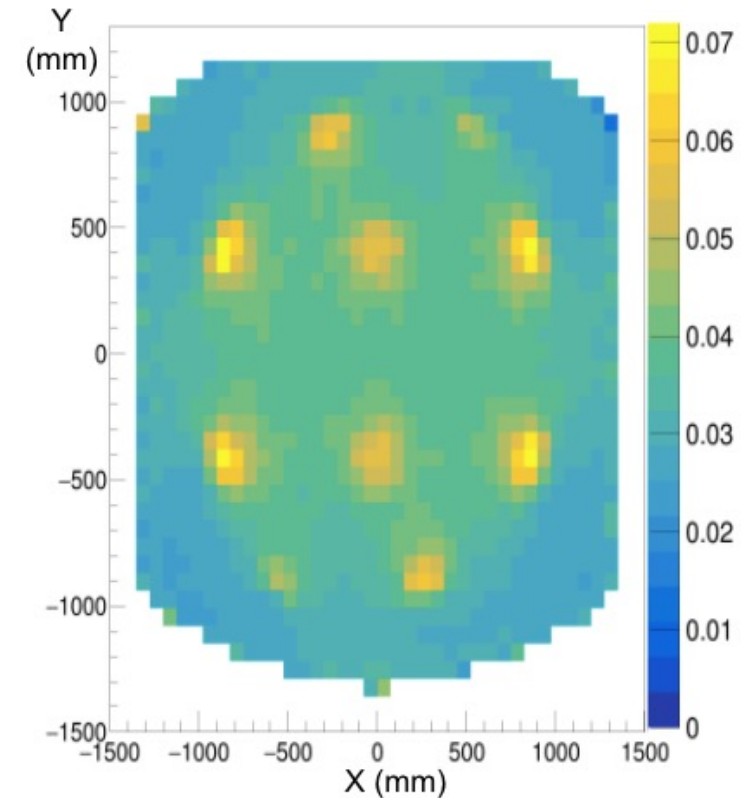
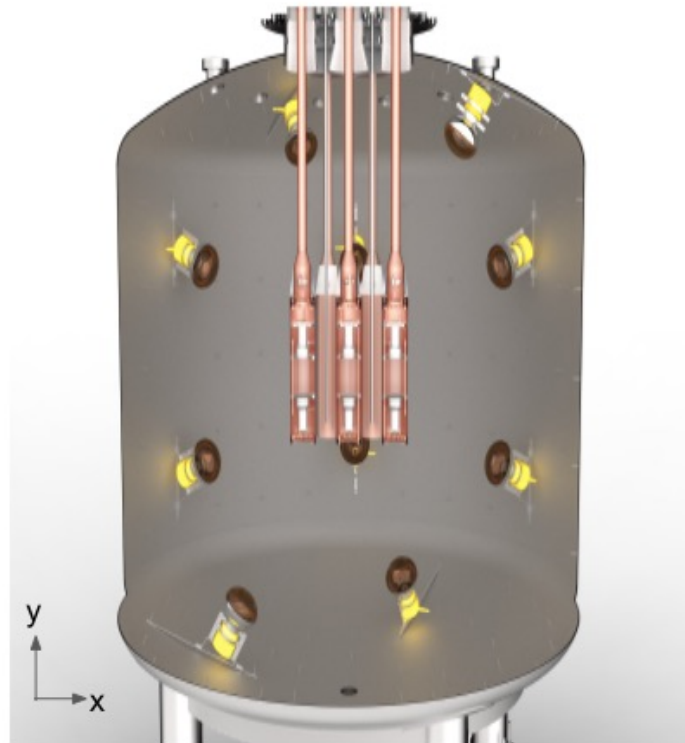
Background simulations assume deposition in scintillator  $\Rightarrow$  detection of optical photon. Not the case!

Successful detection is dependent on

1. Number of photons generated by deposition of energy  $E$ 
  - Light yield of LAB  $\text{Pois}(n; LY \times E)$
2. Probability of photon generated at  $(x, y, z)$  reaching  $\text{PMT}_i$ .
  - Given by  $P_{Di}(x, y, z)$  based on simulation
3. Probability of  $\text{PMT}_i$  detecting photon
  - $QE_i$

True detection probability is:

$$\text{Pois}(n; LY \times E) * \text{Bi}(n, QE_i \times P_{Di}(x, y, z))$$



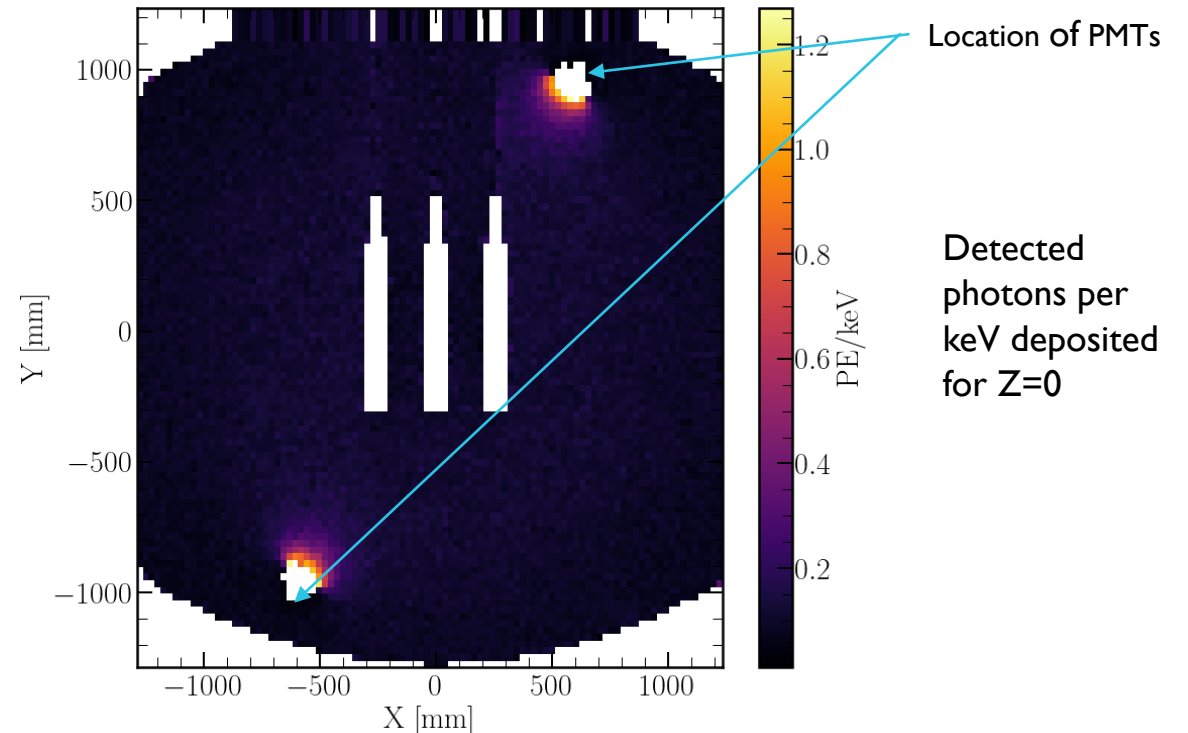
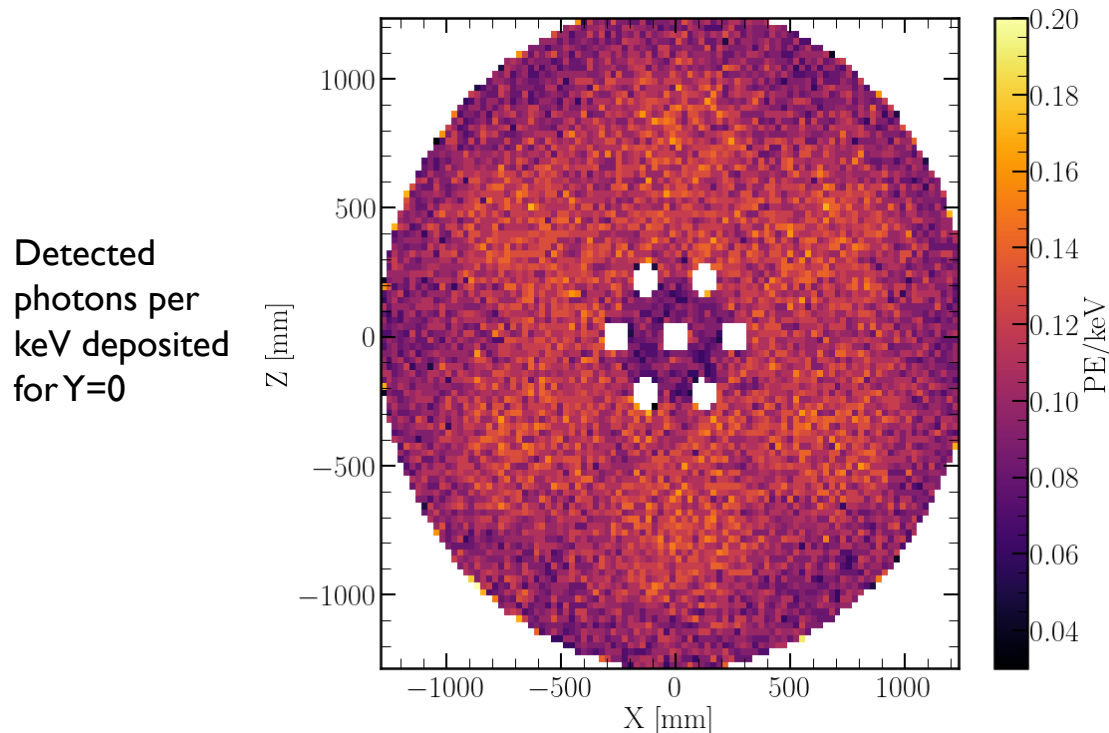
Probability of optical photon hitting PMT as a function of creation position

# ACTIVE VETO SYSTEM

Strong position dependence, but likely we can cut on a lower energy threshold than assumed for simulations (100 keV)

- Average  $P_{Di}(x, y, z) \sim 0.04$
- Average QE  $\sim 0.25$
- Light yield  $\sim 12$  photons/keV

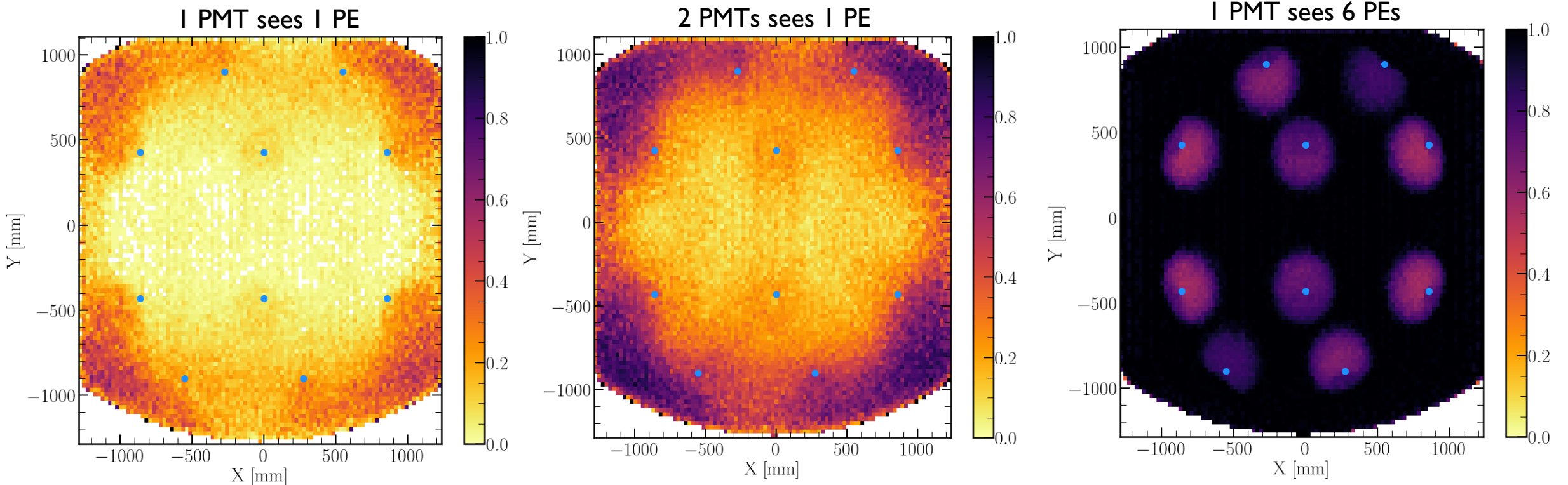
$\Rightarrow$  average number of detections is 12 photons/100 keV, but this can increase by an order of magnitude near PMTs  
(note scale change below)



# ACTIVE VETO SYSTEM

Threshold chosen (number of PEs that define an event) will also impact efficiency as a function of energy and position. Low energy threshold will reduce background and allow for use of LS as detector.

Percentage of hits that will not be registered as a detection (below) increases with stricter thresholds



Fraction of detector deadspace under different threshold conditions for 100 keV deposition. Blue dots indicate PMT positions

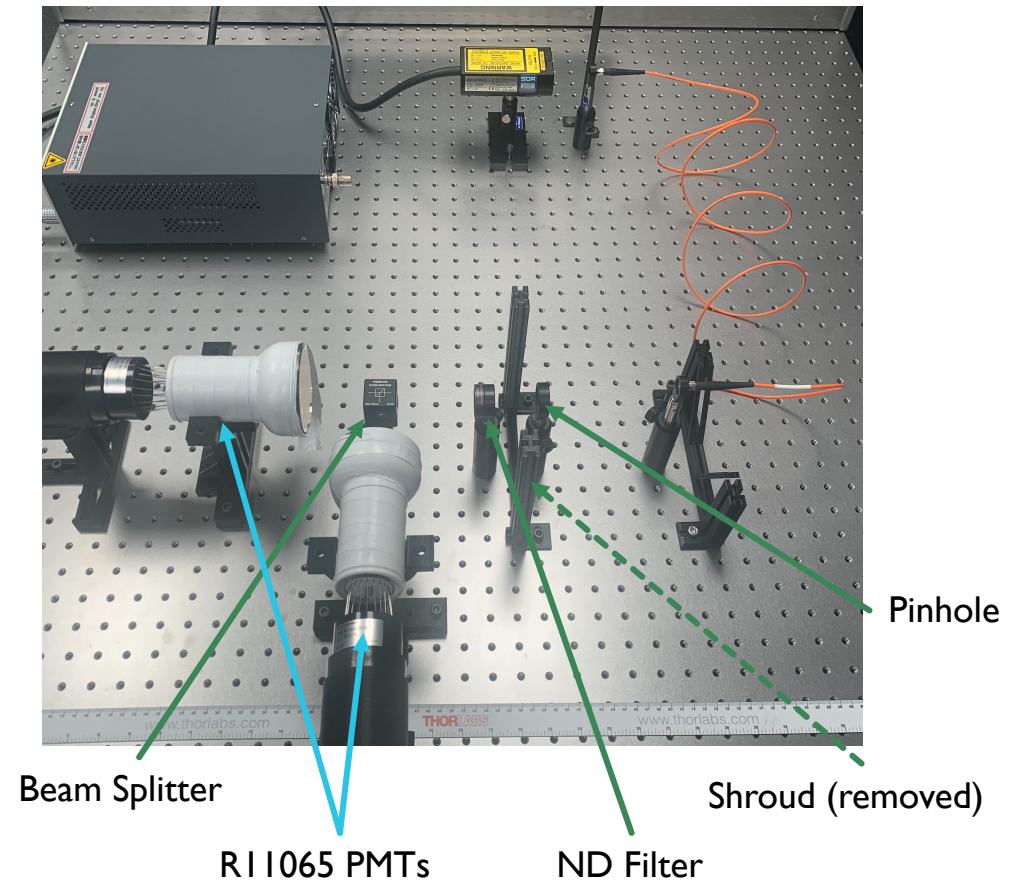
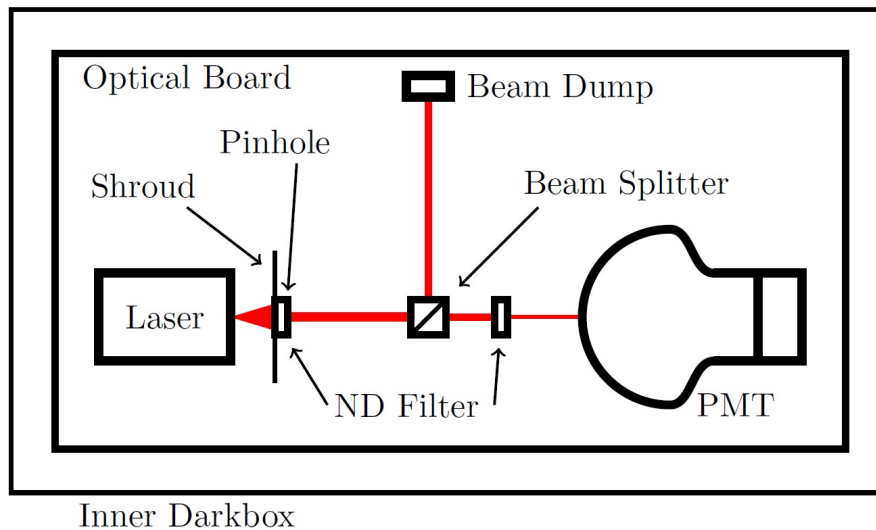
# PMT CHARACTERISATION

To understand achievable thresholds, need to understand PMTs. Characterisation tests have been developed out of Melbourne to understand and model PMT response at this level using a reliable single photon source.

20ps pulsed 405 nm laser.

↓  
Series of ND filters (metallic reflective) and apertures

↓  
Pulses with mean occupancy of 0.1 photons/pulse.

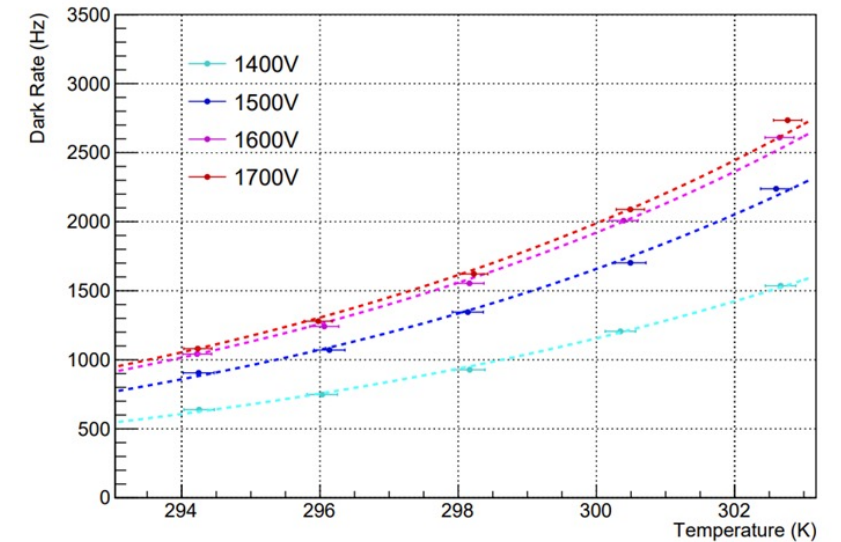
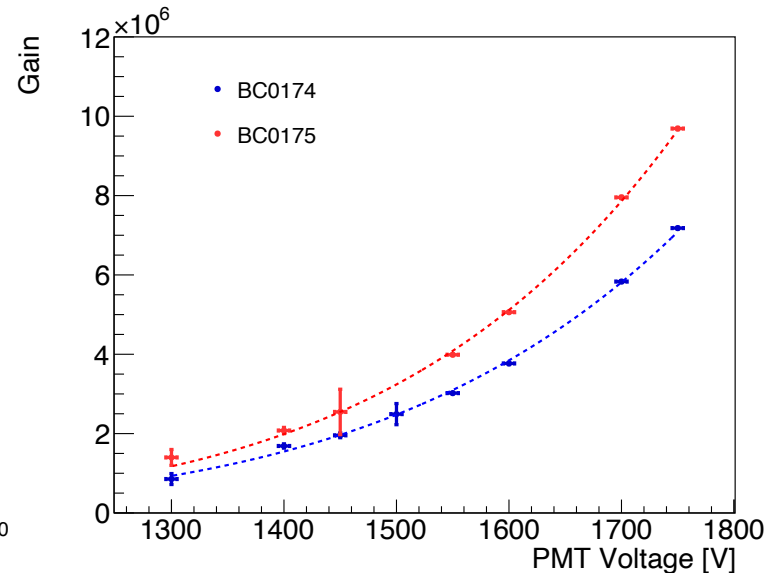
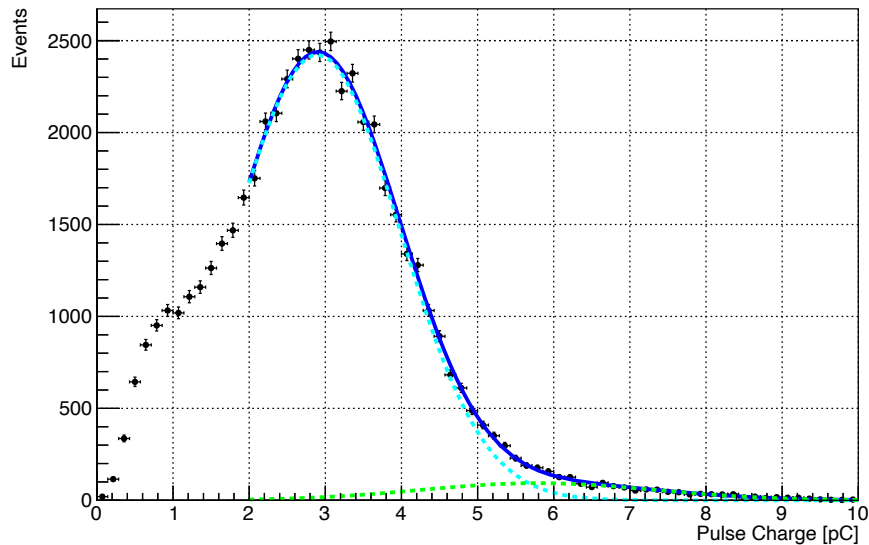


# PMT CHARACTERISATION

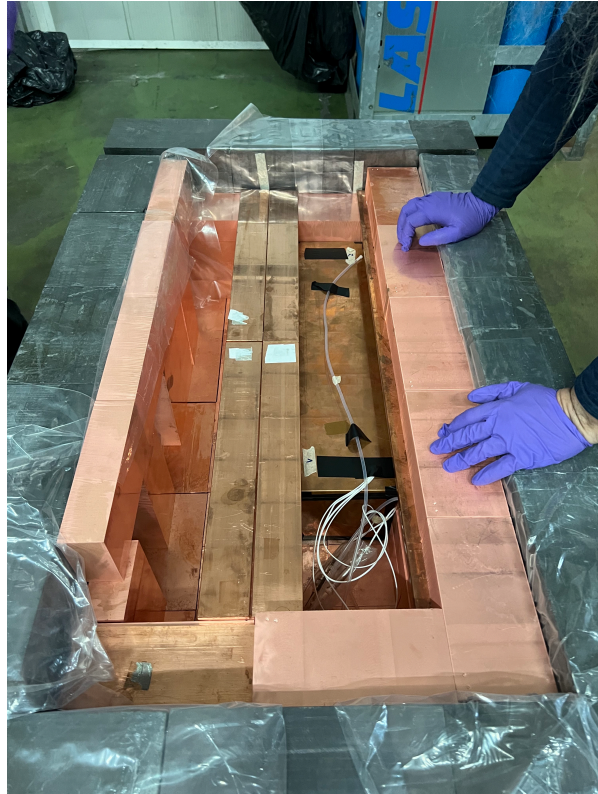
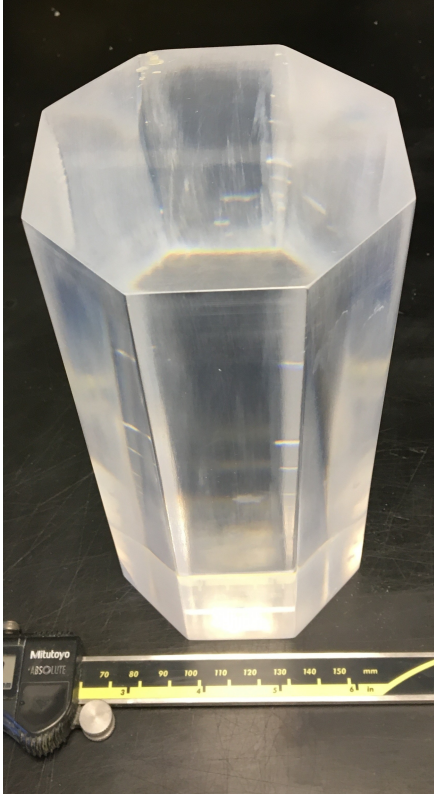
Testing for each individual PMT has commenced. Several key features to be understood:

- Gain/single photoelectron response
- Dark rate
- Temperature dependence
- Quantum efficiency
- Afterpulsing
- Light emission

Fitted PMT Pulse Charge Histogram



# CRYSTAL DETECTOR



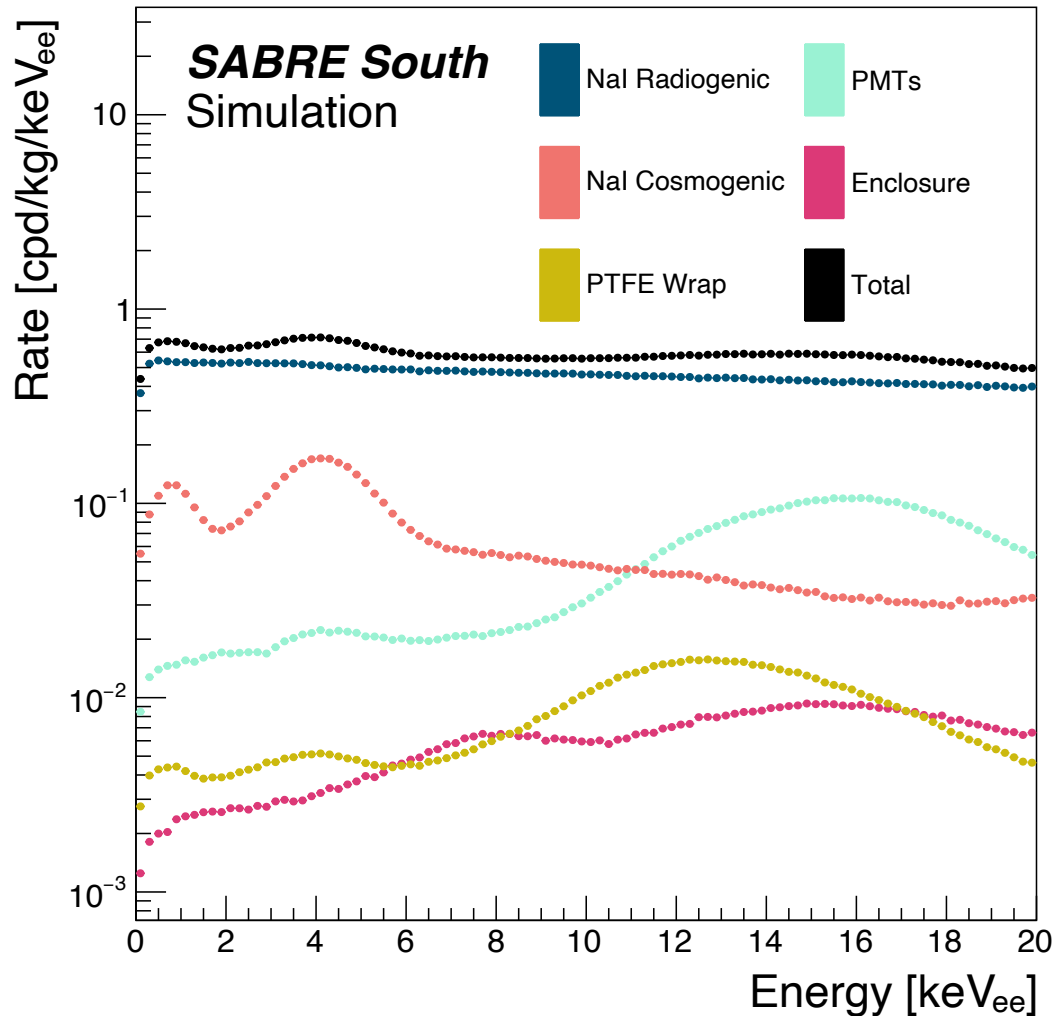
Crystal procurement ongoing, working with RMD and SICCAS. Several SABRE crystals have been characterized at LNGS – have comparable backgrounds to other NaI groups

Crystal	$^{nat}\text{K}$ (ppb)	$^{238}\text{U}$ (ppt)	$^{210}\text{Pb}$ ( $\mu\text{Bq/kg}$ )	$^{232}\text{Th}$ ( $\mu\text{Bq/kg}$ )	Rb in 2-6 keV (cpd/kg/keV)	Active mass (kg)
DAMA [1]	13	0.7-10	5-30	2-31	<0.8	250
ANAIS [2]	31	<0.81	1530	0.4-4	3.2	112
COSINE [3]	<42	<0.12	10-420	7-35	2.7	~60
SABRE [4]	$4.3 \pm 0.2$	0.4	$410 \pm 20$	$1.6 \pm 0.3$	< 1 (goal)	~50 (goal)
PICOLON [5]	<20	-	<5.7	$1.2 \pm 1.4$	< 1 (goal)	~20 (goal)

- [1] R. Bernabei et al., [NIMA 592\(3\) \(2008\)](#)
- [2] J. Amare et al., [EPJC 79 412\(2019\)](#)
- [3] P. Adhikari et al., [EPJC 78 490 \(2018\)](#)
- [4] B. Suerfu et al., [Phys. Rev. Research 2, 013223 \(2020\)](#)
- [5] K. Fushimi et al., [PTEP 4 043F01 \(2021\)](#)



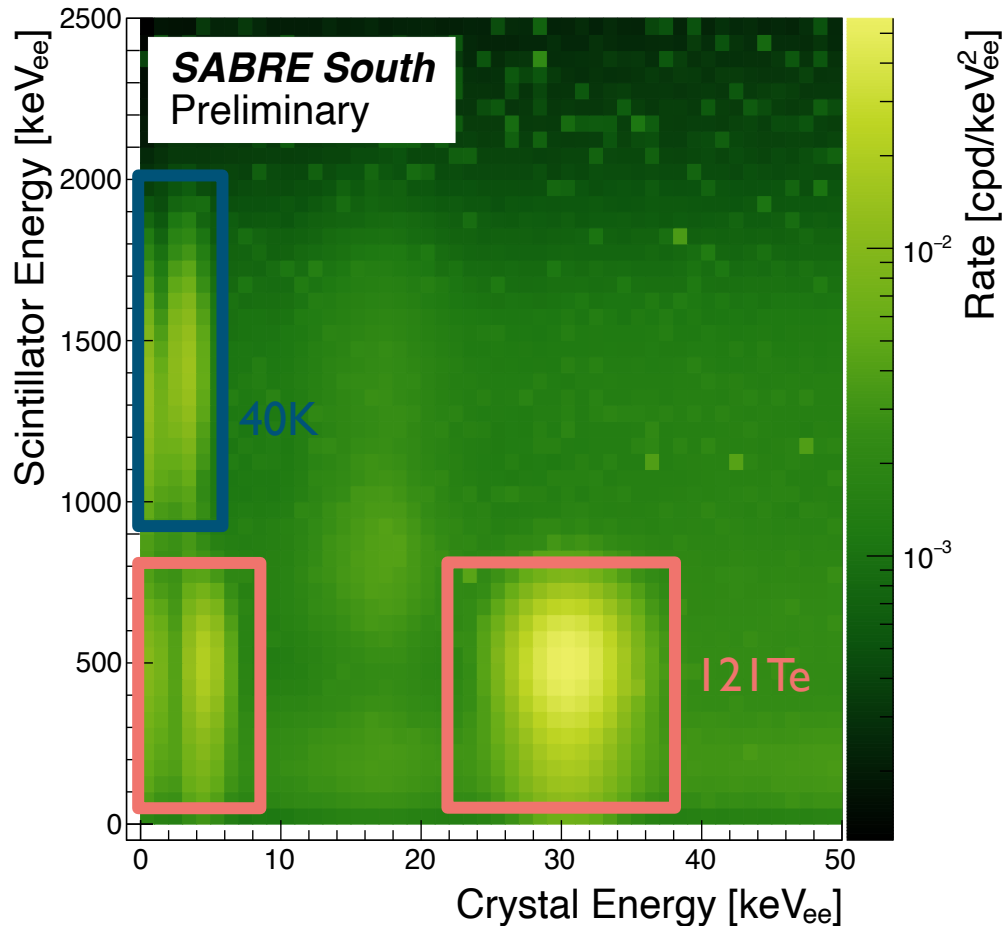
# TOTAL BACKGROUND MODEL



Component	Rate (cpd/kg/keV)	Veto efficiency (%)
Crystal intrinsic	$<5.2 \times 10^{-1}$	13
Crystal cosmogenic	$1.6 \times 10^{-1}$	45
Crystal PMTs	$3.8 \times 10^{-2}$	57
Crystal wrap	$4.5 \times 10^{-3}$	11
Enclosures	$3.2 \times 10^{-3}$	85
Conduits	$1.9 \times 10^{-5}$	96
Steel vessel	$1.4 \times 10^{-5}$	>99
Veto PMTs	$1.9 \times 10^{-5}$	>99
Shielding	$3.9 \times 10^{-6}$	>99
Liquid scintillator	$4.9 \times 10^{-8}$	>99
External	$5.0 \times 10^{-4}$	>93
<b>Total</b>	<b>0.72</b>	<b>27</b>

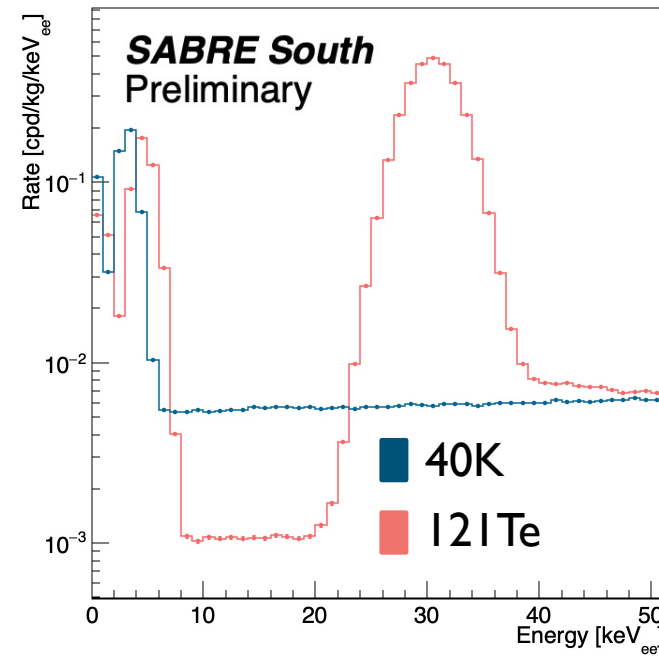
# TOTAL BACKGROUND MODEL

Veto system not only reduces background but also allows for in situ measurements and particle ID.

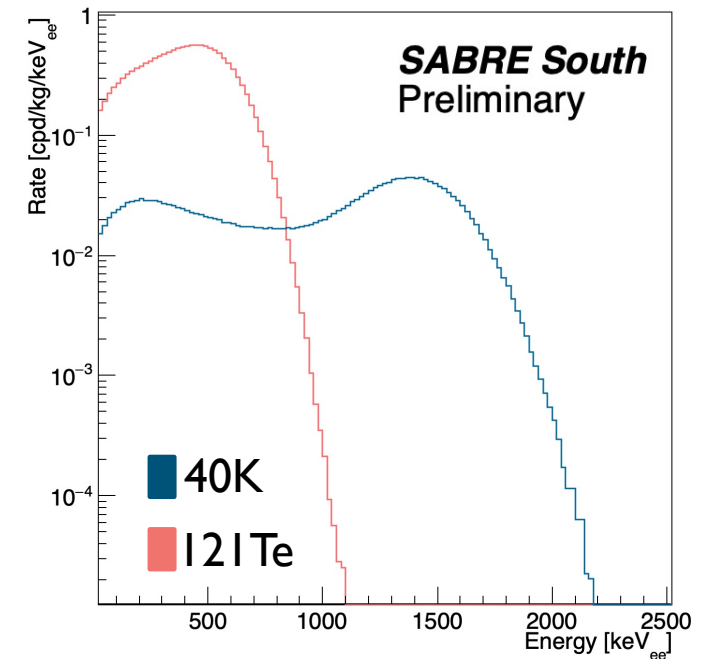


E.g., 40K and 121Te both have distinct islands in crystal-scint energy plane

Rate in crystals

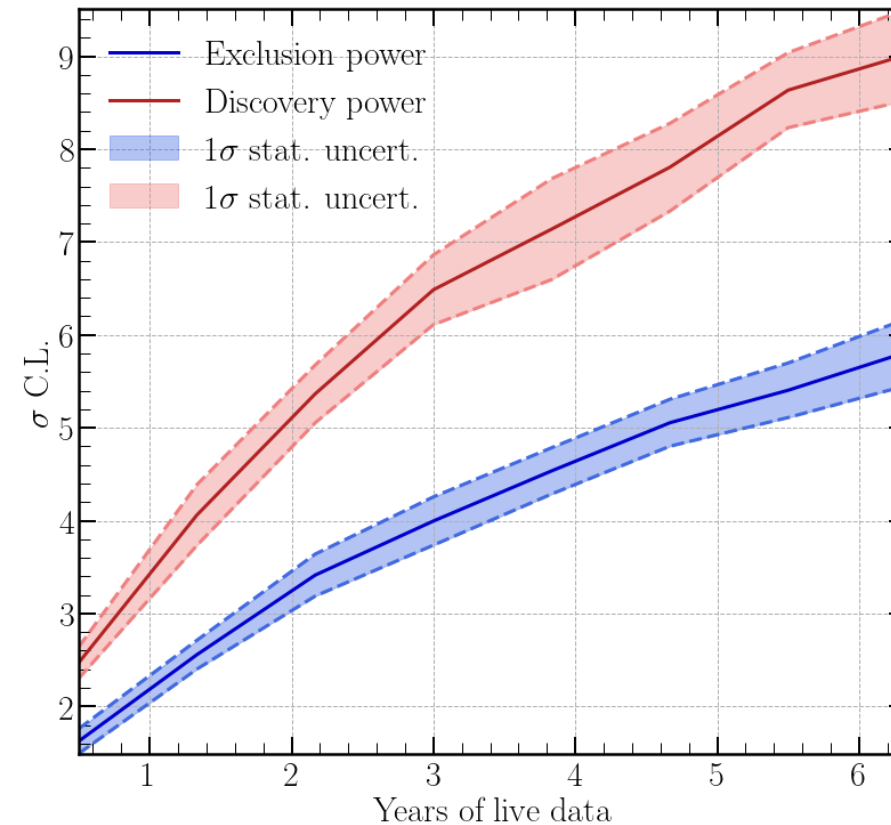
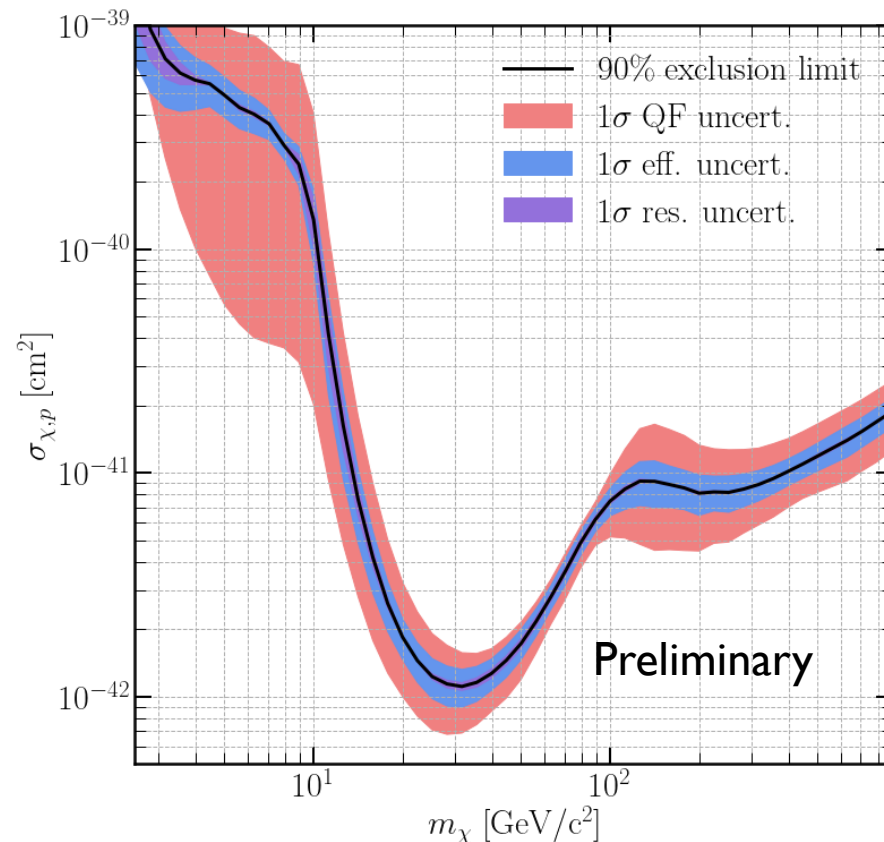


Rate in liquid scintillator



# FUTURE PROJECTIONS

Based on these studies, SABRE South is expected to have a total mass of 50 kg, and background  $\sim 0.7$  cpd/kg/keV. In the event of null results, we should reach  $3\sigma$  exclusion in  $\sim 2$ yr of data taking, and  $5\sigma$  approx 3 yrs after that. In the event of a positive DAMA-like signal, SABRE will have a discovery power of  $5\sigma$  within  $\sim 2$  yrs. Systematic uncertainties will be reduced as the detector is installed and characterised in situ



# FUTURE PROJECTIONS

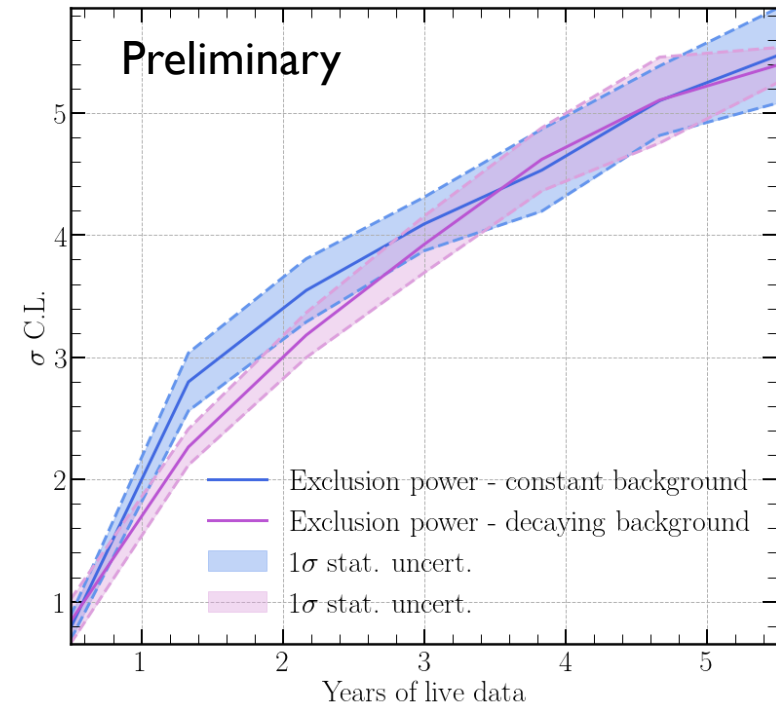
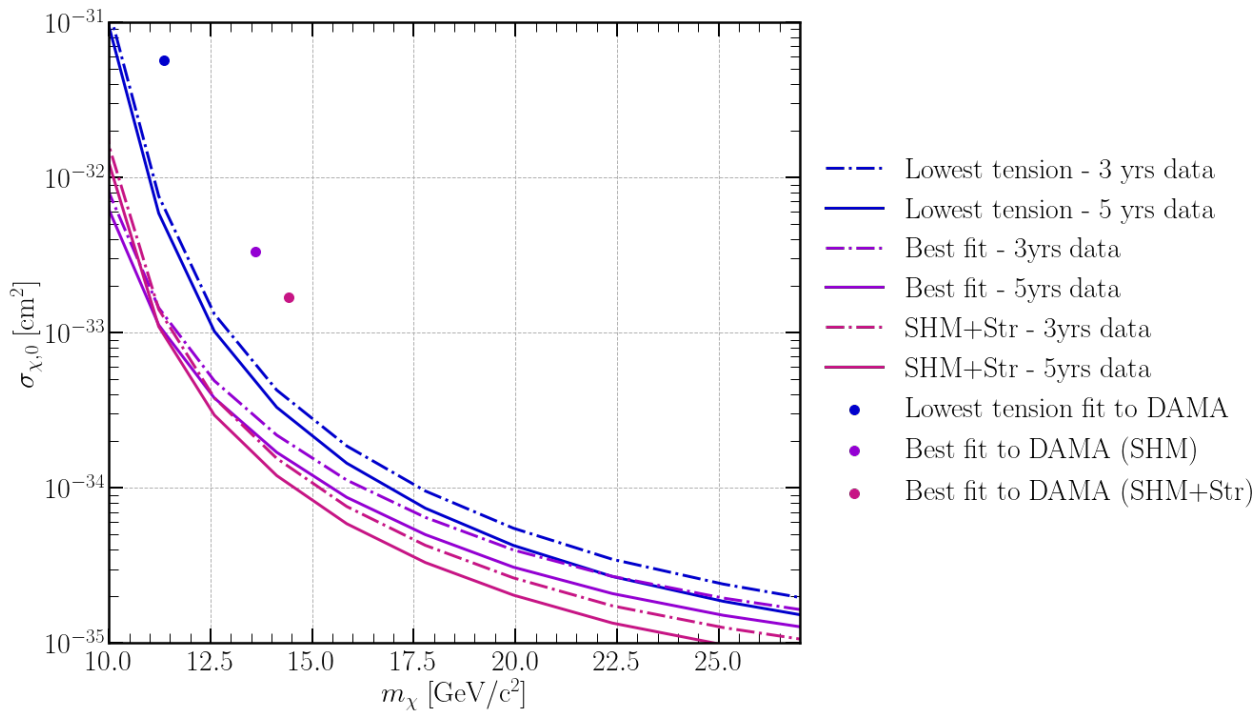
[2] MJZ, Barberio, Busoni JCAP12 (2020) 014

[3] MJZ, Barberio arxiv:2107.07674, EPJC

[1] Kang, Scopel, Tomar, PRD 99, 103019 (2019) [4] Barberio, Duffy, Lawrence, MJZ (in prep.)

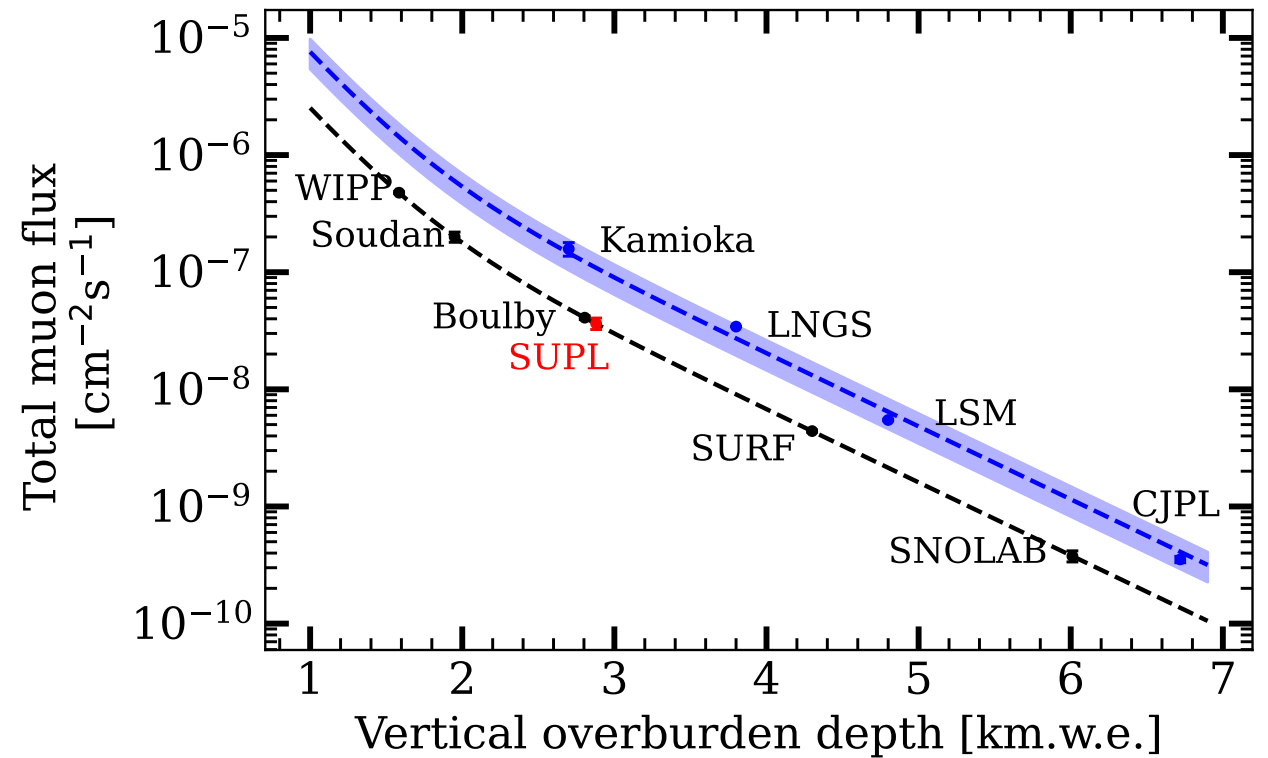
Can also test of influence of different pSIDM models and velocity distributions on fits to DAMA and SABRE sensitivity [1,2,4]

And influence of background models on excluding DAMA [3]

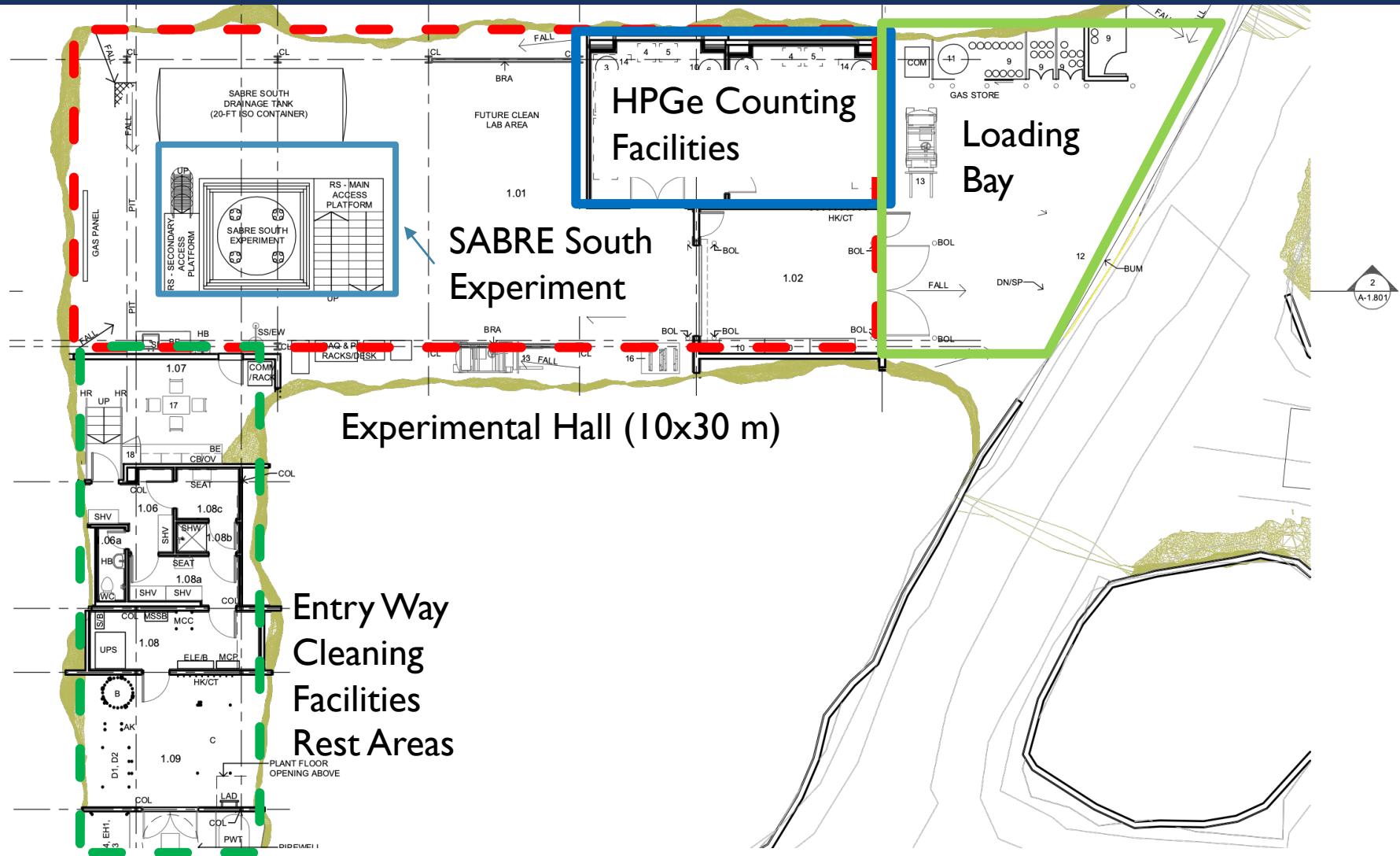


# SUPL STATUS

Stawell Underground Physics Laboratory located in Western Victoria 240 km from Melbourne.  
Lab is 1025 m below ground with flat over burden.



# SUPL STATUS



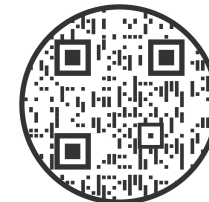
# SUPL STATUS

- SUPL construction completed and handed over at the end of 2022
- Construction and commissioning of the SABRE South experiment at SUPL is starting this year.
- SABRE detectors are now in the process of being moved to SUPL to perform dedicated background measurements during the construction phase



# SUMMARY

- Truly model independent test required to understand DAMA signal
  - Some models exist that can relax experimental tension
  - Must probe modulation rate directly
- This + discrepancies between COSINE and ANAIS motivate an additional low background NaI detector – SABRE
- Differences in detector set up can introduce model dependence
  - Require a low, well characterized background
  - Detector efficiencies and energy threshold can obscure region of interest
  - Resolution may smear signal
  - QF can change where region of interest appears
- Significant work undertaken to reduce the crystal backgrounds, and understand and maximise performance of veto system
- Should SABRE achieve its benchmark goals for mass and background, it will be highly sensitive to a variety of DM models and velocity distributions that might allow for a DAMA-like signal within a few years



Unanswered questions? Contact me:  
Email: [madeleine.zurowski@utoronto.ca](mailto:madeleine.zurowski@utoronto.ca)  
Twitter: @mjzurowski  
Or scan QR code for my details



# ACKNOWLEDGEMENTS



SABRE South



Australian Government



Australian National University



SABRE North



Pacific Northwest  
NATIONAL LABORATORY



SAPIENZA  
UNIVERSITÀ DI ROMA



UNIVERSITÀ  
DEGLI STUDI  
DI MILANO





# BACK UP SLIDES

Poisson simulations are based on expected number of observed interactions:

- Background only:  $N_b = M_E \times \Delta T \times \Delta E \times R_b$
- Signal + background:  $N_{sb} = M_E \times \Delta T \times \Delta E \times (R_b + R_0 + R_m \cos(\omega t))$

Where

- $M_E$  = exposure mass
- $\Delta T$  = data taking time bins
- $\Delta E$  = energy bin widths
- $R_b$  = background rate in energy/time bin
- $R_0$  = constant signal rate in energy/time bin
- $R_m$  = modulating signal rate in energy/time bin

This can be used to compute limits in both a model dependent and independent way:

Model dependent -  $R_0$  and  $R_m$  computed by assuming model, mass and cross section

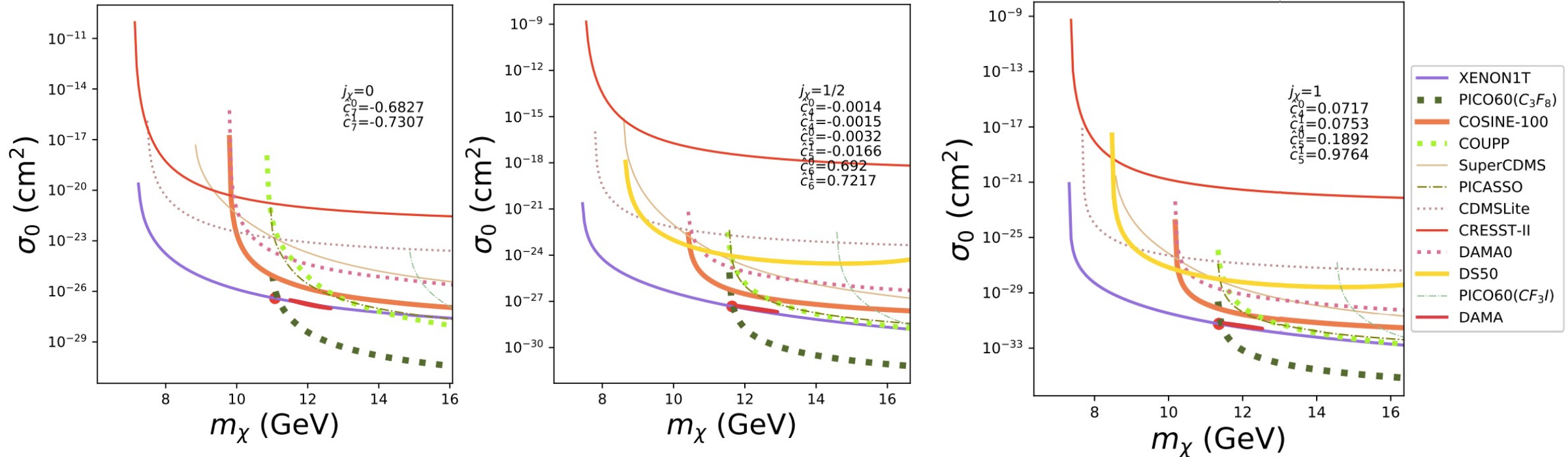
Model independent -  $R_0$  and  $R_m$  taken from measurement by a detector (e.g., DAMA)

# PSIDM MODELS

[1] Kang, Scopel, Tomar, PRD 99, 103019 (2019)

Family of models presented to reduce experimental tension w/ DAMA

Case	Spin ( $j_\chi$ )	$m$ (GeV)	$\sigma_0$ (cm <sup>2</sup> )	$\delta$ (keV)	Non zero $\hat{c}_0$ components	
1	0	11.1	$3.9 \times 10^{-27}$	22.8	$\hat{c}_7^0 = 0.68$	$\hat{c}_7^1 = 0.73$
2	1/2	11.6	$4.7 \times 10^{-28}$	23.7	$\hat{c}_4^0 = -0.0014$ $\hat{c}_5^0 = -0.032$ $\hat{c}_6^0 = 0.692$	$\hat{c}_4^1 = -0.0015$ $\hat{c}_5^1 = -0.0166$ $\hat{c}_6^1 = 0.7217$
3	1	11.4	$5.7 \times 10^{-32}$	23.4	$\hat{c}_4^0 = 0.0717$ $\hat{c}_5^0 = 0.1892$	$\hat{c}_4^1 = 0.0753$ $\hat{c}_5^1 = 0.9764$



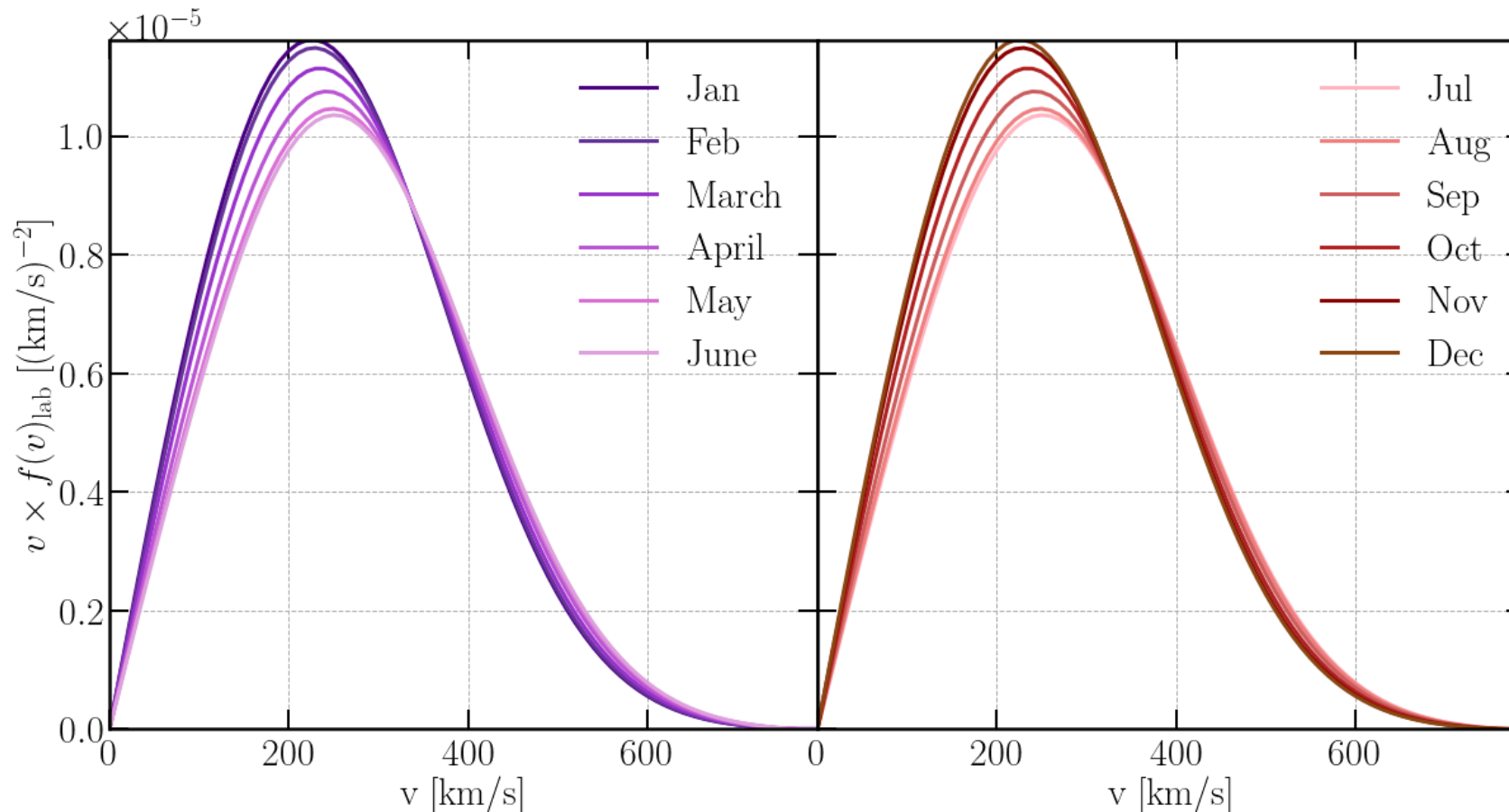
Can take these models and find better fits (rather than the lowest tension)

Also examine influence of velocity distribution – inclusion of high velocity stream substructure increases mass and decreases cross section and mass splitting

Velocity distribution	Model	$m_\chi$ (GeV)	$\sigma_0$ (cm <sup>2</sup> )	$\delta$ (keV)	$\chi^2/\text{dof}$
SHM	1	13.87	$7.53 \times 10^{-29}$	20.17	7.02/12
	2	13.47	$2.09 \times 10^{-29}$	20.82	6.71/12
	3	13.17	$2.45 \times 10^{-33}$	20.42	6.92/12
SHM+Stream	1	14.72	$4.89 \times 10^{-29}$	19.81	7.31/12
	2	14.29	$1.36 \times 10^{-29}$	20.67	6.89/12
	3	13.96	$1.26 \times 10^{-33}$	19.70	7.18/12

# VELOCITY DISTRIBUTIONS

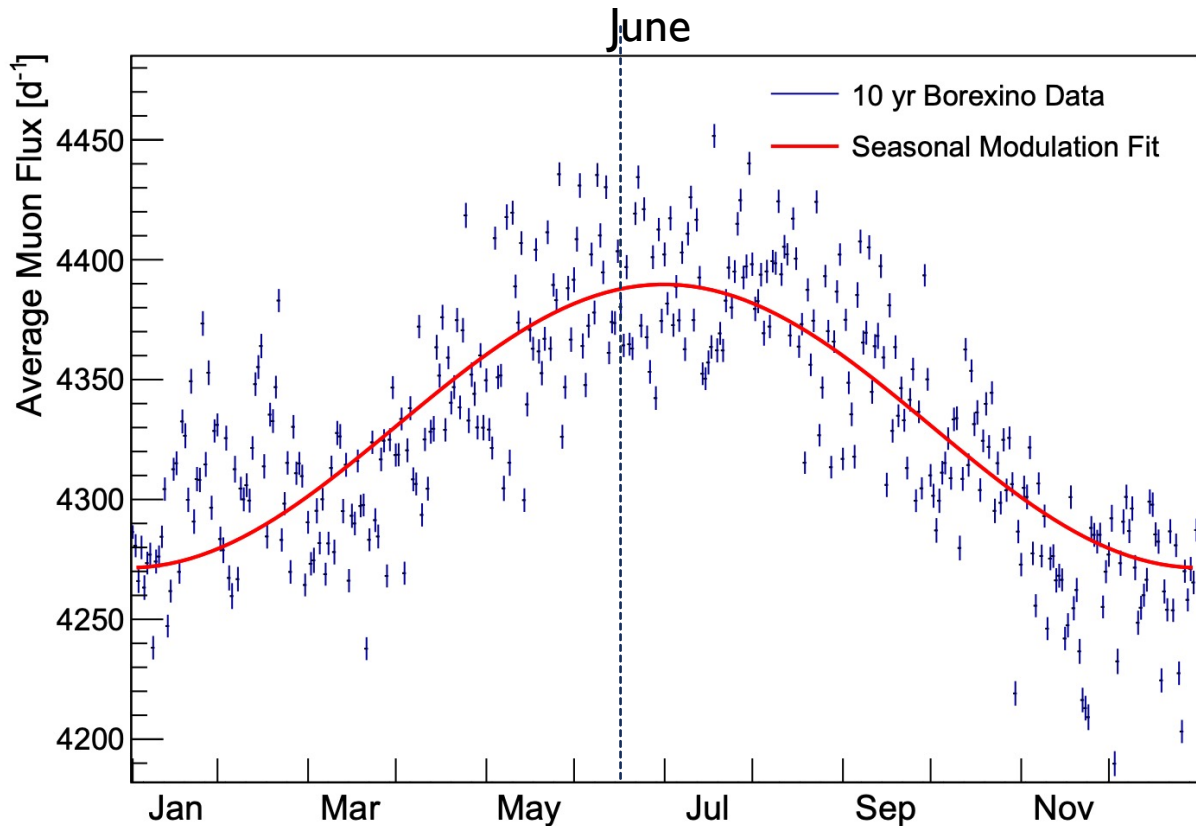
“Negative” amplitude occurs because the velocity distribution is maximized at lower velocities in January, so when integrating over a larger range, and calculating amplitude by taking rate in June and subtracted rate in Jan, you end up with a negative amplitude



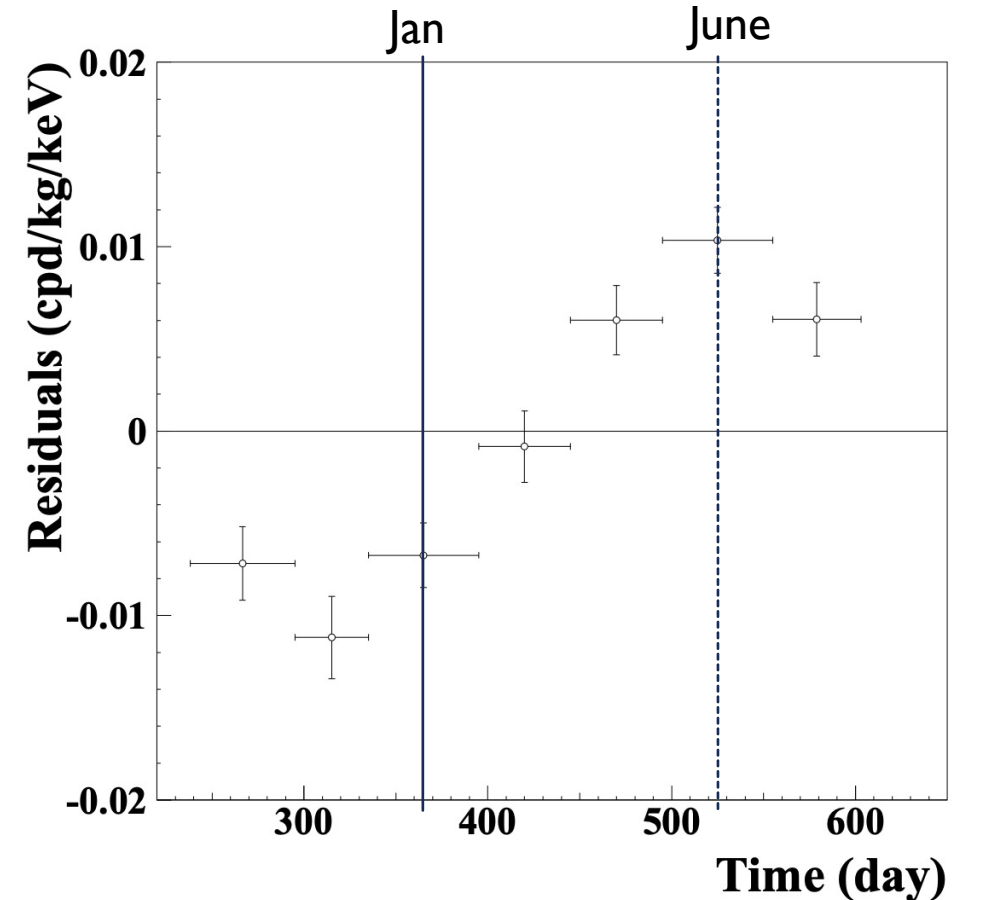
# BACKGROUND MODELS

[1] Borexino collab. JCAP02(2019)046  
[2] DAMA collab. Nucl. Phys. At. Energy 19 (2018)

Muons a particular issue for DM modulation searches as they have a similar phase due to seasonal dependence. Need to be carefully measured to understand their impact on the data.

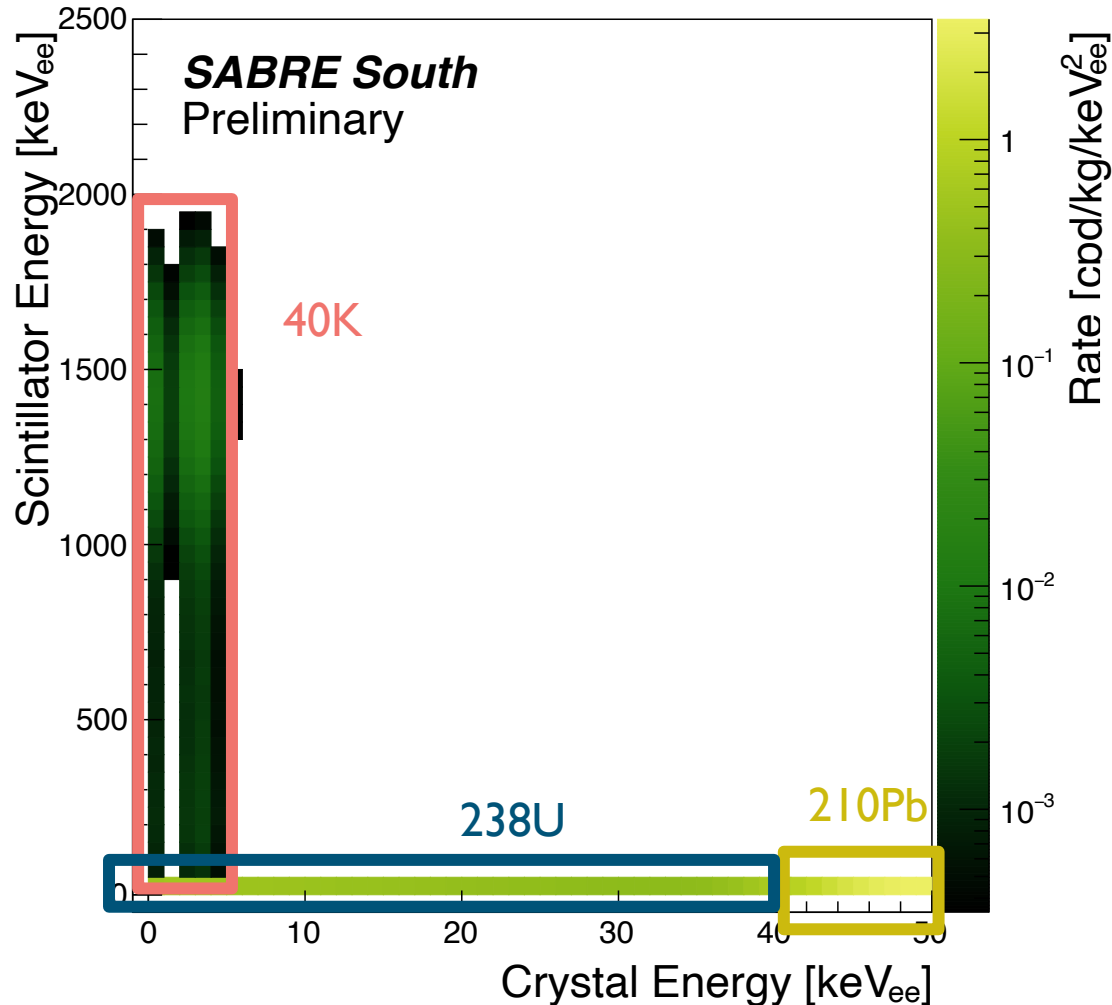


Average muon rate at Borexino over 10 yrs [1]



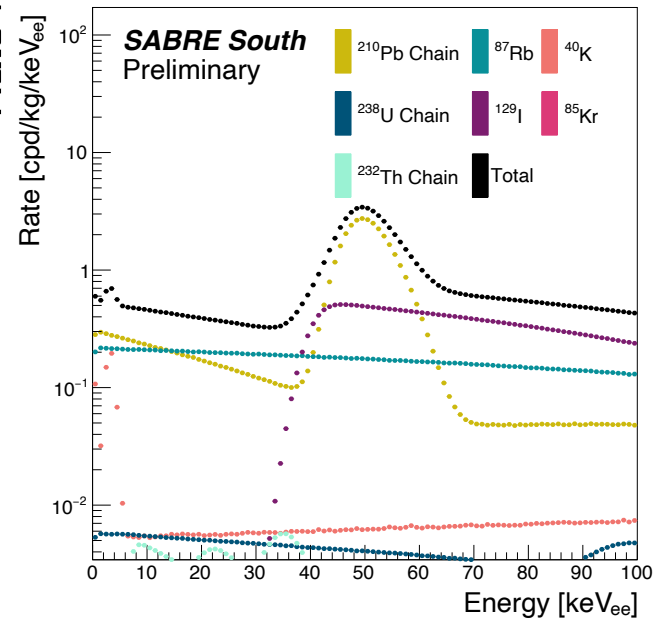
Average modulation at DAMA over 6 yrs [2]

# TOTAL BACKGROUND MODEL

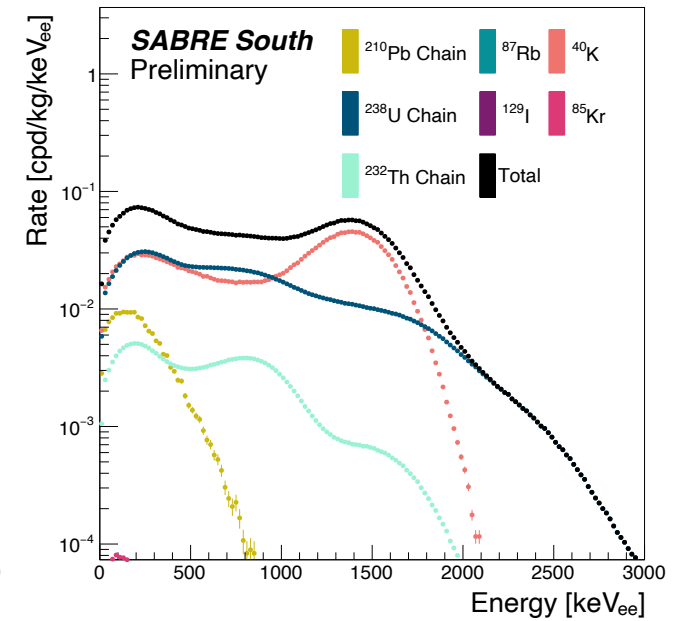


## Contamination from intrinsic radiation of crystals

### Deposition in crystal



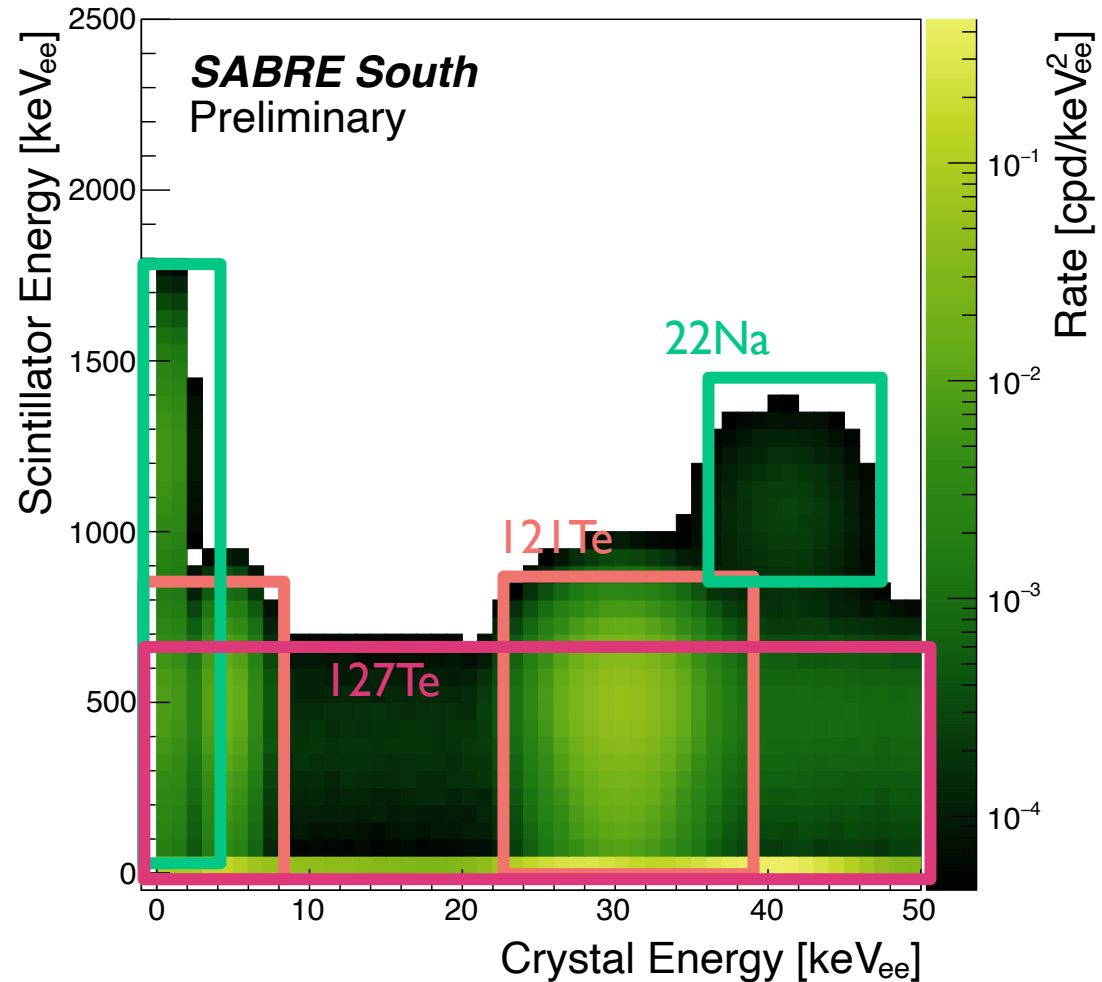
### Deposition in veto





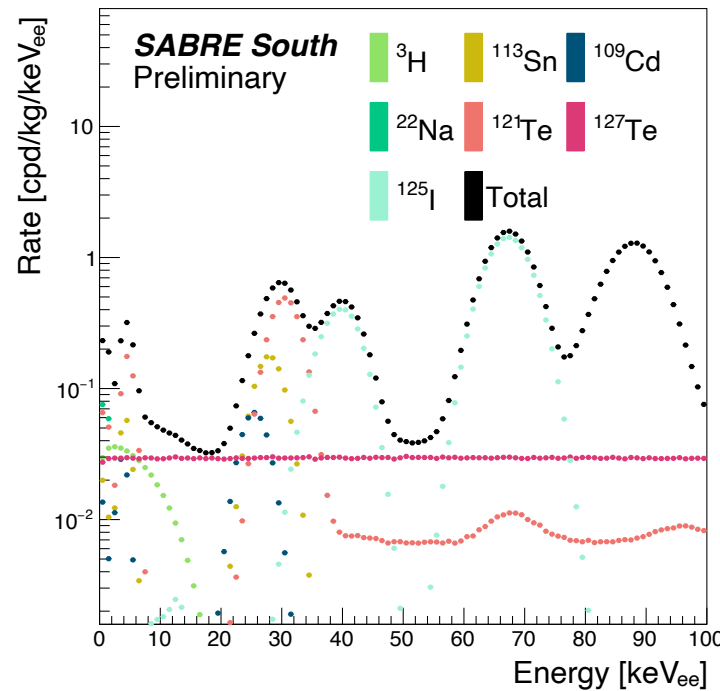
# TOTAL BACKGROUND MODEL

[1] SABRE South Collab. arxiv:2205.13849

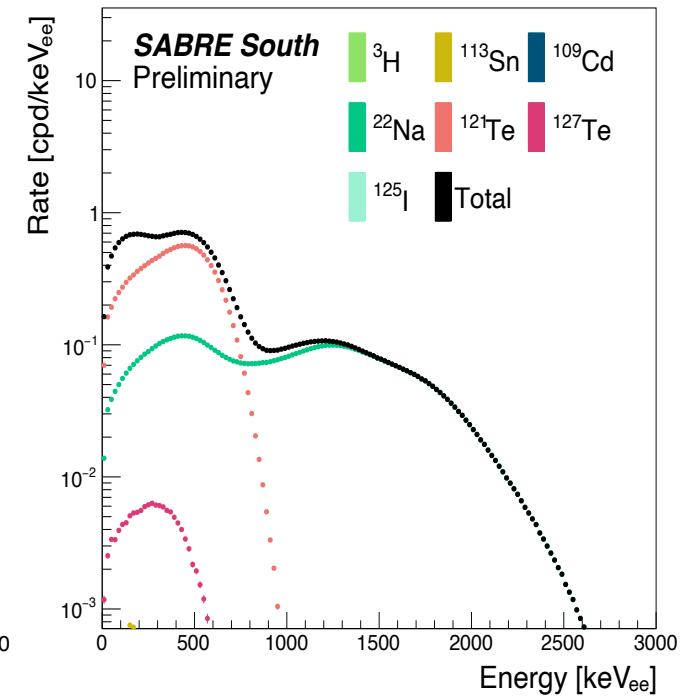


Contamination from cosmogenic activation of crystals

Deposition in crystal



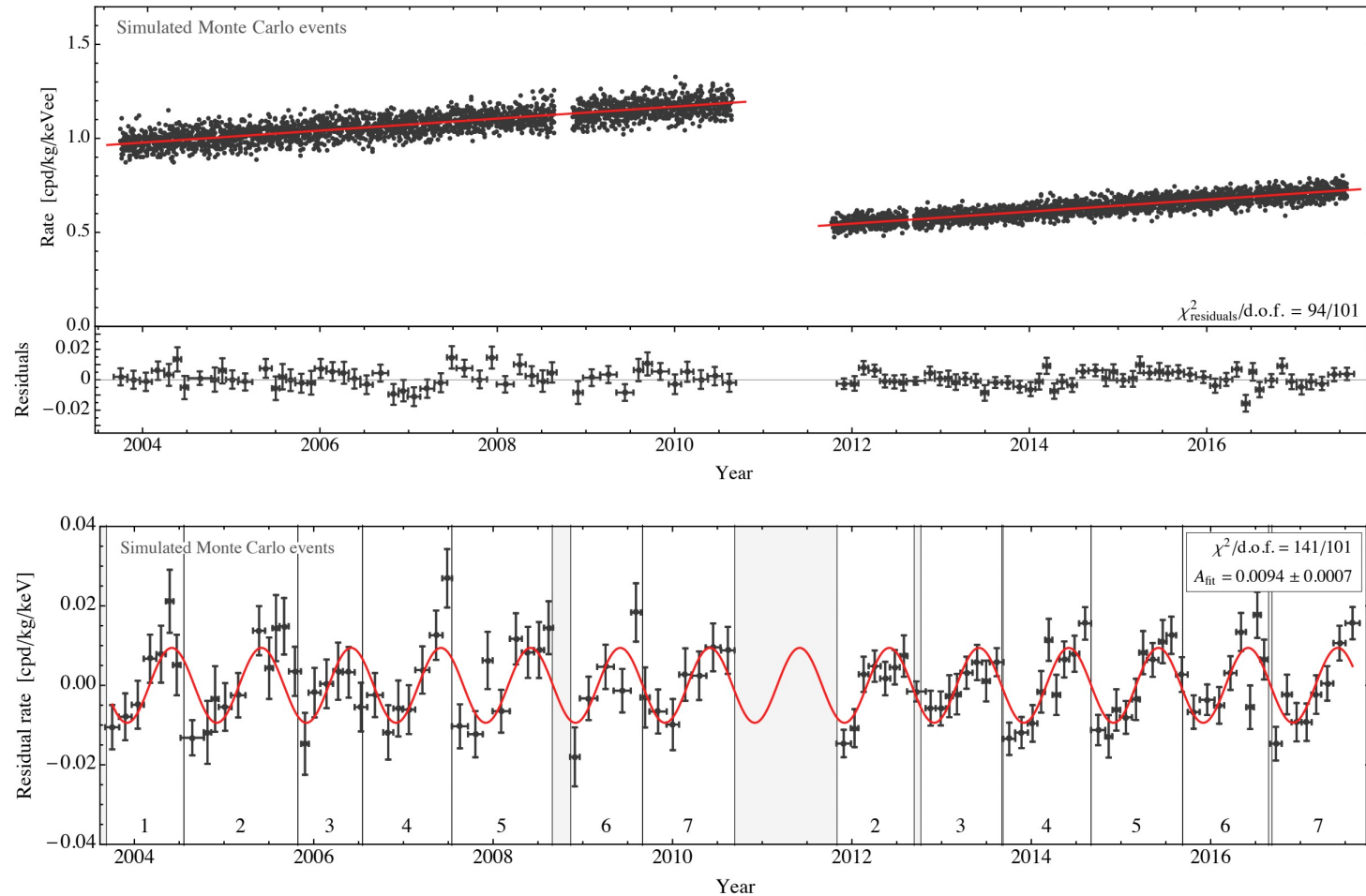
Deposition in veto



# ANALYSIS INDUCED MODULATION

[1] Buttazzo et al JHEP04(2020)137  
[2] Adhikari et al Sci. Rep. 13, 4676 (2023)

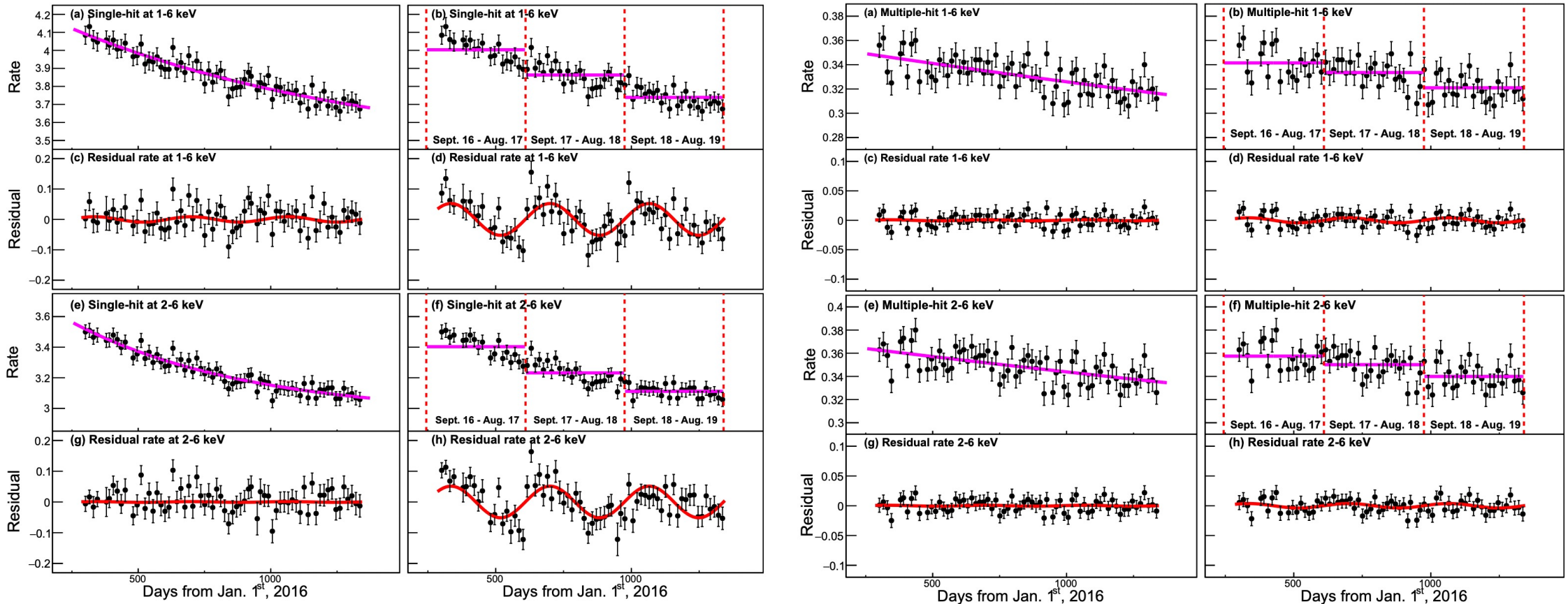
[1] demonstrated the DAMA modulation could be produced by averaging over an increasing background.



# ANALYSIS INDUCED MODULATION

[1] Buttazzo et al JHEP04(2020)137  
[2] Adhikari et al Sci. Rep. 13, 4676 (2023)

[2] performed this analysis with real data from COSINE and saw the expected effect: modulation amplitude equal to DAMA but with phase flip. Interesting note: effect only occurs in the single hit background.





It clear this analysis method introduces a modulation, but to recreate DAMA need either (a) increasing background or (b) very particular start of analysis to produce correct modulation and phase.

The change in background over time needs to be quite drastic, and there is no compelling (at least to me) source for an increase. Reported backgrounds for ANAIS and COSINE also decrease due to cosmogenics, so sensible to assume the same for DAMA, especially give the age and starting purity of detectors.

DAMA have also responded to this [3], stating that their background is effectively constant and that this method cannot explain the modulation given their data.

While I agree with DAMA that this method is unlikely to produce the modulation, I think a more effective refutation is to release their full rate as a function of time (of course this would also help with understanding almost every point I've brought up in this talk).